Modelling for froth flotation control: A review

Paulina Quintanilla*, Stephen J. Neethling, Pablo R. Brito-Parada

Department of Earth Science and Engineering, Royal School of Mines,
Imperial College London, South Kensington Campus, London SW7 2AZ, United Kingdom

Abstract

Flotation is a conceptually simple operation; however, as a multiphase process with inherent instability, it exhibits complex dynamics. One of the most efficient ways to increase flotation performance is by implementing advanced controllers, such as Model Predictive Control (MPC). This type of controller is very dependent on the model that represents the dynamics of the process. Although model development is one of the most crucial parts in MPC, flotation models have been mainly developed for simulation purposes (i.e. analysis and design) rather than control purposes. This paper presents a critical literature review on modelling for froth flotation control. Models reviewed have been sub-classified as empirical, phenomenological and hybrid according to their characteristics. In particular, it is highlighted that models have so far primarily focused on the pulp phase, with the froth phase often neglected; when the froth phase is included, kinetics models such as those used for the pulp phase, are commonly used to represent it. Froth physics are, however, dominated by processes such as coalescence, liquid motion and solids motion, which have been previously modelled through complex, steady-state models used for simulation purposes, rather than control purposes. There remains a need to develop appropriate models for the froth phase and more complex models for the pulp phase that can be used as part of MPC strategies. The challenges associated with the development of such models are discussed, with the aim of providing a pathway towards better controlled froth flotation circuits.

Keywords: Froth flotation, flotation control, flotation modelling, model predictive control

*Corresponding author
Email address: p.quintanilla18@imperial.ac.uk (Paulina Quintanilla)

Contents

1. Introduction

Froth flotation is the largest tonnage separation in mineral processing by which valuable mineral is separated from waste rock. Advances in control and optimisation of the froth flotation process are of great relevance since even very small increases in recovery lead to large economic benefits (Ferreira and Loveday, 2000; Maldonado et al., 2007a). However, the implementation of advanced control and optimisation strategies is not always completely successful in flotation. This is because flotation performance is affected by a great number of variables that interact with each other (Arbiter and Harris, 1962; Laurila et al., 2002), while unmeasurable disturbances in the process further complicate the implementation of efficient strategies (Cubillos and Lima, 1997).

Froth flotation is affected by several variables, such as the flowrates into the flotation cell, i.e. feed, air and froth wash water, as well as the addition rate of the various chemical reagents; the slurry density and solids content as well as the slurry level in the tank; electrochemical potentials such as pH, Eh and conductivity; ore mineralogy and the size, distribution and liberation of the particles; the bubble size distribution and the velocity and stability of the froth; and the mineral concentration in the feed, concentrate and the tailings (Laurila et al., 2002). In terms of process control, these variables are classified as manipulated, disturbance, controlled, and internal state variables.

Manipulated variables are defined as those that can be modified to change the internal states of the model; disturbance variables are those that cannot be modified or controlled and, only in some cases, can be measured or estimated; controlled variables are the objective of the control; and state variables are internal variables that define the models (Sbarbaro and del Villar, 2010). Particularly for flotation, control variables are usually classified as follows (Hodouin, 2011; Jovanović et al., 2015; Shean and Cilliers, 2011) (as shown in Fig. 1):

- Inputs (or independent variables):
  - Manipulated variables: air flowrate, reagent addition rate, tailings flowrate, feed mass florwate, wash water flowrate (specially in columns), frother addition rate.
  - Disturbances: particle size distribution, solids content, head grade, volumetric flowrate, particle properties (size distribution, mineralogy, shape, degree of liberation), froth properties, electrical potentials in the pulp (i.e. pH and Eh).
- Outputs (or dependent variables):
  - Controlled variables: pulp level, froth depth, grade, gas hold-up.
  - Internal states: froth properties, such as bubble size, bursting rate, coalescence rate, particle settling velocity, liquid content, among others. For intermediate cells: grade, recovery, total solids, flowrates, mass pull.

It is worth mentioning that there tend to be discrepancies in the classification of flotation control variables. For example, Lynch et al. (1981) considered the reagent addition points and the concentrate collection points as manipulated variables. These variables, however, are likely part of the circuit design and should not be considered as manipulated variables

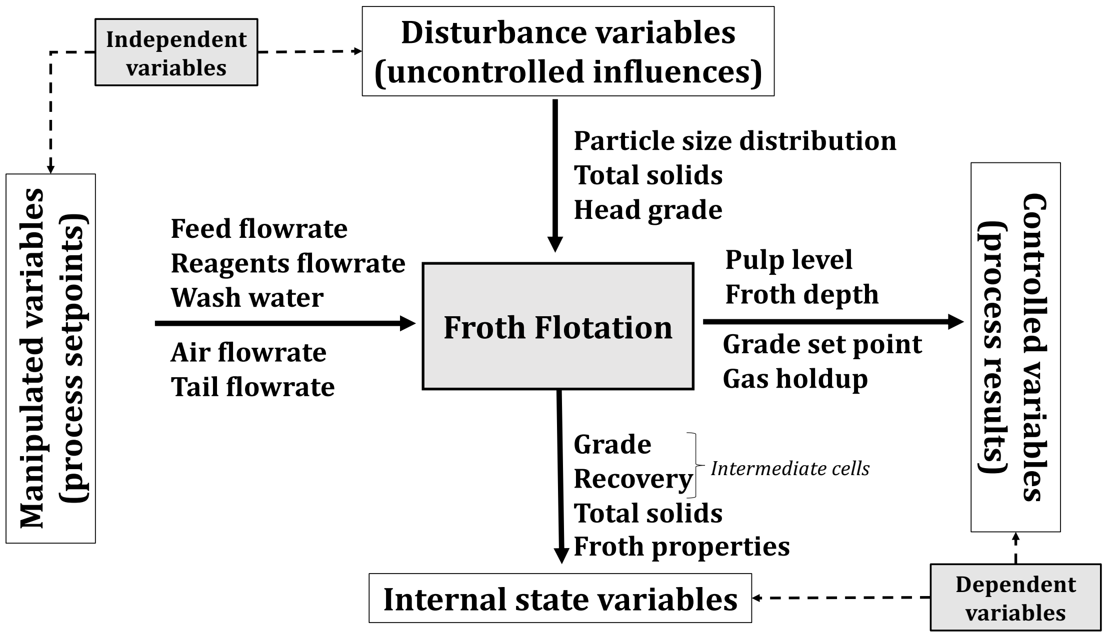

Figure 1: Classification of flotation variables. (Adapted from Lynch et al. (1981); Hodouin (2011); Jovanović et al. (2015))

for control purposes (Oosthuizen et al., 2017). Another discrepancy is that the target for concentrate grades in the intermediate cells, in some cases, could be also considered as a controlled variable.

It must also be noticed that for some researchers, such as Lynch et al. (1981) and Hodouin (2011), pulp level set point in each cell or bank is considered a manipulated variable, while others (Bergh and Yianatos, 1994; Laurila et al., 2002) define the pulp level set point as a controlled variable, since it changes as a consequence of manipulating the tailings flowrate and air flowrate, instead of being directly manipulated. Tailings flowrate may be also set as a ratio of the cell feed flowrate and, thus, the concentrate flowrate can be defined if no wash water is added. A summary of the control variables used in the studies discussed in this literature review manuscript is shown in Table A1, in the Appendix.

It should also be noted that with improved process instrumentation some of the control variable categories may change. Problems with the available instrumentation may be considered as one of the biggest challenges at industrial scale (Laurila et al., 2002; Carr et al., 2009; Shean and Cilliers, 2011; Bergh and Yianatos, 2011), and it could directly affect the performance of any type of controller. For example, Bergh and Yianatos (1996, 2003) stated that accurate on-line estimation of concentrate grades using an XRF analyser, generally demands a significant amount of work in maintenance and calibration. Additionally, Bergh and Yianatos (2003) also highlight that in a number of flotation plants worldwide, the concentrate grade and recovery data usually have a large variability. It must be emphasised, however, that this literature review is not focused on instrumentation itself, and the reader is referred to Laurila et al. (2002) and Shean and Cilliers (2011) for a full description of instrumentation in froth flotation plants.

The most conventional controller is the so-called Proportional-Integral-Derivative (PID), which has been widely used in many types of processes, including froth flotation. PIDs are often used as regulatory controllers and are designed to maintain the most important operating variables in their set points. Although PIDs have been considered as a robust strategy for regulatory control, its performance decreases when the process is under disturbances that continuously change the optimal operating conditions. This problem arises from the fact that PIDs do not explicitly use a process model nor constraints, making it more difficult to adapt to changes. Another disadvantage of PID controllers is their high sensitivity to the interaction between process variables. For processes with very complex dynamics, as is the case of froth flotation, PIDs are not sufficient to maintain the plant in its optimal conditions as it is a SISO controller (single-input single-output) and, therefore, only one controlled variable can control one manipulated variable, neglecting the effect of interactions from the other process variables.

These problems can be addressed by complementing the PIDs (regulatory control) with advanced control techniques, such as expert control systems, based on image analysis, Artificial Neural Networks (ANN), Fuzzy Logic (FL), and Model Predictive Control (MPC), among others. In particular, it has been widely accepted that MPC is one of the advanced control techniques that is capable of dealing with complex processes, such as froth flotation, due to its ability to cope with multivariable systems, considering several process constraints (Desbiens et al., 1994, 1998; Bouchard et al., 2009; Sbarbaro and del Villar, 2010; Bergh and Yianatos, 2011). The MPC technique is addressed in more detail in Section 2.

Expert control systems are based on human experience, using heuristic rules, and knowledge-based or expert opinions. The main idea of this type of controller is to take adequate decisions and control the process by imitating the reasoning from experts (Jovanović and Miljanović, 2015). Flotation control strategies have been implemented as expert systems to control metallurgical objectives (i.e. grade and recovery), via the manipulation of froth depth, air flowrate and wash water flowrate set points (Mckay and Inchausti, 1996; Bergh and Yianatos, 1996; Bergh et al., 1999). Expert controllers are commonly implemented as an alternative in the absence of mathematical models required by other types of advanced controllers (Bergh et al., 2013), and they can also form a higher level control on top of more conventional control strategies. However, these controllers have some disadvantages as they are based on decision making on local set points between steady states, without considering either the process dynamics or process constraints (Bergh and Yianatos, 2003; Bergh et al., 2013). Their efficiency is still debatable and their performance could be improved if robust and sufficient instrumentation were available (Shean and Cilliers, 2011).

Advanced flotation controllers based on froth image analysis have been developed in recent years. Machine vision can, for example, determine some characteristics of the froth surface at the top of a flotation cell, such as the number of bubbles, bubble size, bubble shape, density, speed and stability (Fu and Aldrich, 2019). Aldrich et al. (2010) classified process control strategies that are based on image analysis into four groups: (i) based on the appearance of the froths to take specific control actions (Moolman et al., 1994, 1995a,b,c,d, 1996; Cipriano et al., 1998; Holtham and Nguyen, 2002; Wang et al., 2003; Bartolacci et al., 2006); (ii) based on froth features that allow operating conditions in the process to be inferred (Niemi et al., 1997; Hyötyniemi and Ylinen, 2000; Ventura-Medina and Cilliers, 2000; Bonifazi et al., 2001; Citir et al., 2003); (iii) based on the detection of rare behaviour in the process and its consequent adjustment by using “process maps” or “control charts” that are capable of identifying the nature of the problem (Liu et al., 2005); and (iv) based on the use of image variables as input for classical control strategies (Bartolacci et al., 2006; Liu and MacGregor, 2008; Jahedsaravani et al., 2016; Riquelme et al., 2016). Although image analysis techniques have numerous advantages such as their consistency across all cells monitored, the possibility of linking to plant data, and a high frequency of measurements (Forbes, 2007), some features, such as the estimation of mineral concentration in the froth phase have not been fully implemented yet at industrial scale (Aldrich et al., 2010; Fu and Aldrich, 2019). For a comprehensive literature review on the topic of online monitoring and control for flotation, the reader is referred to Aldrich et al. (2010).

An artificial neural network (ANN) is a mathematical structure that is used to identify relationships between input and output data that have complex, nonlinear characteristics (Hsu et al., 1995). In the case of flotation, models to represent relevant phenomena by using ANN have been proposed (Gupta et al., 1999; Al-Thyabat, 2008; Mohanty, 2009; Chelgani et al., 2010; Massinaei and Doostmohammadi, 2010). For flotation control, models based on ANN must be capable of maintaining operating conditions that yield the desired metallurgical objectives, i.e. recovery and/or concentrate grade, through the adequate manipulation of the system's set points (Shean and Cilliers, 2011). Gupta A., Yan D.S. (2006), for example, carried out a study based on ANN modelling to control the collector addition rate in order to maintain the recovery set point, while Cubillos and Lima (1997), implemented hybrid-neural modelling, a schematic of which is shown in Figure 2, for both adaptive identification and optimisation of the flotation system, using models at steady state. Although the number of adjustable parameters (network weights) needed to develop models based on neural networks are few compared to other systems, there are still issues related to the possibility of over-fitting due to the many associated degrees of freedom, as well as to the availability of sufficient appropriate training data.

Fuzzy logic (FL) control is based on knowledge gained by experience that is represented by numbers between 0 and 1 (Gupta A., Yan D.S., 2006), depending on the degree of truth. The relationship between variables, in terms of process control, can be written using "*IF-THEN*" logical rules. Fig. 3 shows a schematic of the fuzzy control strategy. A number of different FL based control strategies have been discussed in the literature (Bergh et al.,

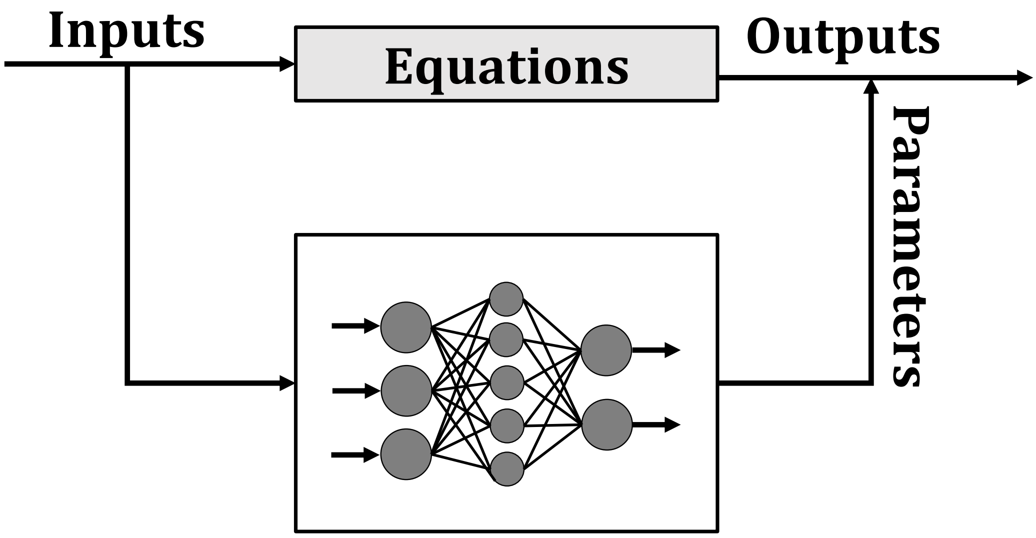

Figure 2: Schematic representation of the hybrid neural modelling technique. Adapted from Cubillos and Lima (1997)

1998; Osorio et al., 1999; Hodouin et al., 2001; Liao et al., 2011), with these being tested using simulators. A recent example of FL control applied in a flotation system is the study carried out by Jahedsaravani et al. (2016), in which an FL controller for a batch-flotation system was designed using empirical data and froth images. Parameters were calibrated by evaluating the system behaviour at several discrete operating conditions due to the lack of reliable dynamic flotation models suitable for control purposes.

While Jahedsaravani et al. (2016) report that satisfactory results were obtained, there still remains a need for an efficient method that can deal with a large number of parameters without the need for these to be manually tuned (Lewis, 1997), since this makes FL a very time-expensive type of controller (Bergh et al., 1998).

To deal with the complex dynamics of the flotation process, a major focus on model-based predictive controllers (MPC) has been undertaken, generating considerable recent research

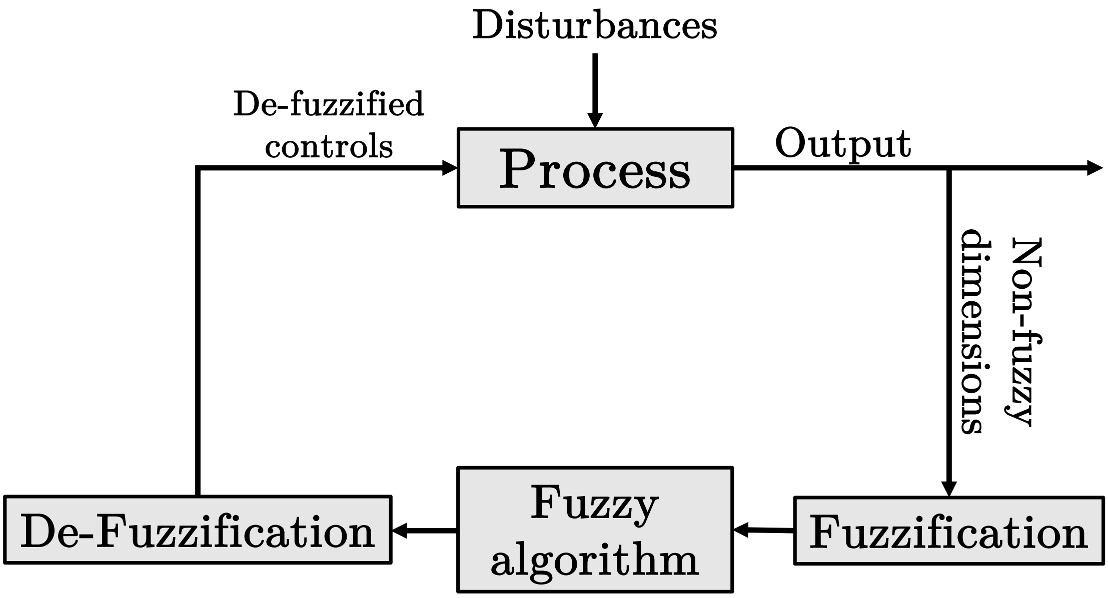

Figure 3: Schematic representation of fuzzy control (Adapted from Gupta A., Yan D.S. (2006)).

interest. As previously mentioned, MPC is ideal for implementing in multivariable processes such as froth flotation, in which several process constraints must be taken into account (Desbiens et al., 1994, 1998; Bouchard et al., 2009; Sbarbaro and del Villar, 2010; Bergh and Yianatos, 2011). The most crucial part of MPC strategies is the model development itself (Desbiens et al., 2000; Maldonado et al., 2009; Sbarbaro and del Villar, 2010; Bergh, 2016), which must ensure that models accurately describe non-linear processes, such as those occurring in flotation (Hodouin et al., 2001). Flotation modelling is a particularly difficult task as it is affected by a great number of variables to different extents (Arbiter and Harris, 1962; Laurila et al., 2002), as well as due to its complex dynamics caused by the interaction between phenomena in both the pulp and froth phases (Neethling and Brito-Parada, 2018).

A number of literature reviews focused on flotation control have been published in recent years, though none of these has focused on either model-based controllers or the dynamic modelling required when implementing such strategies. For example, an overview of process control in the mineral processing industry - including key aspects for the flotation process - was presented by Hodouin (2011); while an overview of control and simulation implemented specifically in flotation columns can be found in Bouchard et al. (2009). In the latter, a sub-classification of flotation models was made according to their use, as those used for (i) models to predict recovery, (ii) models to study the dynamics of the process, and (iii) models used as soft sensors. Nonetheless, whereas Bouchard et al. (2009) mentioned the most important models used in flotation column studies, no further analysis of models used for flotation control was made. Shean and Cilliers (2011), on the other hand, discussed advanced control strategies implemented in mechanic flotation cells. Another literature review on flotation control is that of Jovanović et al. (2015), in which the hierarchical levels in flotation control, with an emphasis on model predictive control and intelligent control (expert control and machine vision), were discussed.

The aim of this manuscript is, therefore, to critically analyse and classify, for the first time in the literature, the existing froth flotation models that are amenable to be used for control purposes, as well as to highlight the modelling areas that require further research to be effectively implemented into MPC strategies.

The analysis of the literature reveals that the most commonly used models for MPC are the empirical models, which have demonstrated good performance at laboratory and pilot-plant scale. However, the presence of disturbances that continuously change the process conditions means that the process can move beyond the conditions over which the models were originally calibrated. Purely empirical models thus typically perform badly when extrapolating to predict performance. A wider range of disturbances can be reliably predicted by implementing phenomenological models. Most of the existing phenomenological models are based on the kinetics of the flotation process, assuming well-mixing conditions or plug flow, and have been used to represent both the pulp and froth phases. While kinetic descriptions provide good approximations for pulp phase behaviour, they are not adequate to model froth phase behaviour.

The froth phase is neither close to being well mixed nor plug flow conditions, with complex relative motions between phases. This is further complicated by the influence of bubble coalescence and bursting, which is hard to predict due to its complex interrelationship with the flotation chemistry, particle properties and flow behaviour. The importance of including the froth phase into control strategies is that froth stability is related to the mobility of the froth, and therefore, to the overall solids recovery. Additionally, bubble size in the froth determines the amount of water recovered in the concentrate, which is directly linked to the entrained solids, and thus, to the concentrate grade.

In the following section, a brief overview of Model Predictive Control (MPC) is presented for a better understanding of this strategy, as well as to provide insight into the importance of modelling for control purposes.

2. Model Predictive Control

Model-based predictive control (MPC) is a wide set of different strategies that have in common the use of an explicit model of a process and the minimisation of an objective function (Camacho and Bordons, 2007) to maintain the controlled variables at the desired set-point with optimal trajectories. All MPC strategies need to have: (1) a prediction model, (2) an objective function, and (3) a control law. The prediction model is, in fact, the most crucial part of MPC. This model must represent the dynamics of the process as accurately as possible and, at the same time, it must be simple enough to be solved in the shortest possible time.

The general form of the objective function is given in Eq.(1), in which the future output ($\hat{y}$) should follow a given reference trajectory (r), and the necessary control changes (Δu), which can be weighted, as follows:

$$J\left(N_1, N_2, H_c\right) = \sum_{j=N_1}^{N_2} \omega(j)[\hat{y}(t+j|t) - r(t+j)]^2 + \sum_{j=1}^{H_c} \lambda(j)[\Delta u(t+j-1)]^2, \tag{1}$$

where N_1 and N_2 are the minimum and maximum prediction horizons, H_c is the control horizon. The coefficients $\omega(j)$ and $\lambda(j)$ are functions that consider the future behaviour. This coefficients can be set to cover a wide range of control options, from smoother control to tighter ones (Camacho and Bordons, 2007). $r(t+j)$ is the reference trajectory. The control law is obtained by minimising the objective function (Eq.(1)) in order to calculate the values for the control u.

The objective functions of different MPC strategies that have been developed for flotation are shown in Table 1. As can be seen, these objective functions can vary from the general form presented in Eq.(1) in different ways. For example, Zaragoza and Herbst (1989) used an economic approach as objective function. This economic approach considered the price of the copper (P_{Cu}), a penalty for concentrate grade less than a constraint value (P_{pen}), and the reagent costs (i.e. price for the frother (P_{Fr}) and collector (P_{Co})). Additionally, their objective function considered also performance aspects, such as the metallurgical recovery (R), the concentrate grade (g), and the operating variables: copper mass flowrate (M_{Cu}), frother flowrate (M_{Fr}) and collector flowrate (M_{Co}).

A structure more similar to that of Eq.(1) is found in Putz and Cipriano (2015). In this case, they considered the final tailings grade ($y_4(k)$) as output, which must follow a given reference ($r(k)$). The changes in the position of output control valves ($\Delta u_1(k), \Delta u_2(k), \Delta u_3(k)$) was also considered in their objective function. A similar approach was taken by Maldonado et al. (2007a) and Maldonado et al. (2009). In their objective function, while the tracking error (i.e. the difference between the trajectory ($\hat{r_j}(k+i/k)$) and the predicted controlled variables ($\hat{y_j}(k+i/k)$ were weighted by the term w_j, the control changes on the manipulated variables ($\Delta u_p(k+i)$) over the control horizon H_c, were weighted by the term λ_p. In addition, Maldonado et al. (2007a, 2009) added a third term to the objective function ($\rho_j \nu_j$) in order to "soften the output constraints" (Maciejovski, 2002). In Maldonado et al. (2007b) the objective function was stated as the minimisation of the tailings copper grade in each bank. However, although the tailings grade ($g_{T_{Cuj}}$) is generally easy to measure, it must be noted that maximising recovery by reducing the tailings grade could be considered as an oversimplification of the economic maximisation calculation.

Camacho and Bordons (2007) describe several advantages that MPC has over other control strategies:

- Tuning is reasonably easy, particularly for non-trained personnel, since control con-

Table 1: Objective functions used in MPC strategies for the flotation process.

Study	Objective function
Zaragoza and Herbst (1989)	$J = P_{\mathrm{Cu}} \cdot RM_{\mathrm{Cu}}^{F} - P_{\mathrm{pen}} \cdot (g_{\mathrm{pan}} - g) - P_{\mathrm{Fr}} \cdot M_{\mathrm{Fr}} - P_{\mathrm{Co}} M_{\mathrm{Co}}$
Perez-Correa et al. (1998)	$J = \sum_{i=1}^{p} \hat{e}'_{k+i} \Gamma \hat{e}_{k+i} + \sum_{i=1}^{C} \Delta u'_{k+i-1} \Lambda \Delta u_{k+i-1}$
Maldonado et al. (2007a, 2009)	$J = \sum_{j=1}^{N_y} \sum_{i=H_S}^{H_P} \left\{ w_j \cdot (\hat{r}_j(k+i/k) - \hat{y}_j(k+i/k))^2 \right\} + \sum_{p=1}^{N_u} \sum_{i=0}^{H_C-1} \lambda_p \Delta u_p(k+i)^2 + \sum_{j=1}^{N_y} \rho_j \nu_j^2$
Maldonado et al. (2007b)	$J = Q \left(g_{\mathrm{CC}_N} - \widehat{g}_{\mathrm{CC}} \right)^2 + R \sum_{j=1}^{N} g_{T_{\mathrm{Cy}}}^2$
Putz and Cipriano (2015)	$J = \sum_{i=0}^{N-1} \Vert y_4(k+i+1 \mid k) - w(k+i \mid k) \Vert_Q^2 + \Vert \Delta u_1(k+i \mid k) \Vert_R^2) + \Vert \Delta u_2(k+i \mid k) \Vert_p^2 + \Vert \Delta u_3(k+i \mid k) \Vert_S^2)$
Tian et al. (2018)	$J = \sum_{j=0}^{N-1} [< x(z, k+j \mid k), Qx(z, k+j \mid k) \rangle + < \bar{u}(k+j+1 \mid k), R\bar{u}(k+j+1 \mid k) >] + < x(z, k+N \mid k), \bar{Q}x(z, k+N \mid k) >$

cepts are very intuitive;

- it can be used in any kind of process, even those with complex dynamics or which are unstable;
- it can be used as a multivariable controller;
- it has intrinsic delay compensation; and
- plant constraints can be simply included during the design of the controller.

A reliable dynamic model is needed to implement an MPC strategy. Dynamic models, of the form presented in Eq.(2), are needed as they allow the prediction of future plant responses under given operating conditions (Bergh and Yianatos, 2011):

$$\frac{d\mathbf{x}}{dt} = f(\mathbf{x}, \mathbf{u}, \mathbf{w}, \boldsymbol{\theta}, t), \tag{2}$$

where $\mathbf{x}$ is the vector of states, f is a set of nonlinear process functions, $\mathbf{u}$ is the inputs vector, $\mathbf{w}$ is the process noise vector and $\boldsymbol{\theta}$ is the model parameters vector (Herbst et al., 1992). In the case of flotation, conservation of mass usually forms the basis for the dynamic models. Modelling for flotation control is extensively reviewed in Section 3 in this paper.

An MPC strategy can be carried out through the implementation of models to predict the future response of the plant over a finite time horizon. This finite control horizon is used to apply the first control signal, as well as to repeat each of the following steps, by using new measured variables (Camacho and Bordons, 2007; Bordons, 2000), as follows:

1. At each instant t, the outputs of the process are predicted by using the plant model proposed for a given horizon H_c.

2. For $j = N_1 ... N_2$ the predicted outputs $\hat{y}(t + j|t)$ (this notation refers to the value of the variable at instant t+j that is predicted at instant t) depend on the known values from the past (up to t) and on the future control signals $u(t + j|t)$ for j=0...$(H_c - 1)$ that are calculated and sent to the system.

3. The objective function is optimised by staying as close as possible to the "reference trajectory" ($r(t{+}j)$), which refers to the set point (or an approximation of it).

4. Step 1 is repeated when the next sampling instant $y(t + 1)$ is known. The control signal $u(t|t)$ is sent to the process, while the future control signals are discarded.

Fig. 4 presents the basic structure of an MPC implementation. While models of the process are used to predict the future plant outputs based on the proposed future control signals, the optimisation is done by minimising a cost function and considering plant constraints based on manipulated and/or controlled variables (Camacho and Bordons, 2007; Maciejovski, 2002; Rossiter, 2003; Veselý and Rosinová, 2010). The control signals are calculated according to the optimisation cost function and plant constraints; if inequality constraints exist, numerical methods with more calculation load are needed. In general terms, MPC strategies differ from each other in the particular models used to describe the process, how disturbances are estimated, and the cost function used to optimise the process (Camacho and Bordons, 2007).

Although MPC has had some successful implementations at industrial scale, specially in petrochemical plants (Qin and Badgwell, 1997), it has not been effectively implemented in every industry due to the need to have relatively simple, dynamic models of the process (Bordons, 2000) that are accurate enough to represent the process behaviour. Minerals processing is not an exception in terms of lack of implementations of MPC, and it is particularly challenging for froth flotation as it has complex dynamics that are difficult to be accurately represented using simple models. While detailed flotation models have been developed for

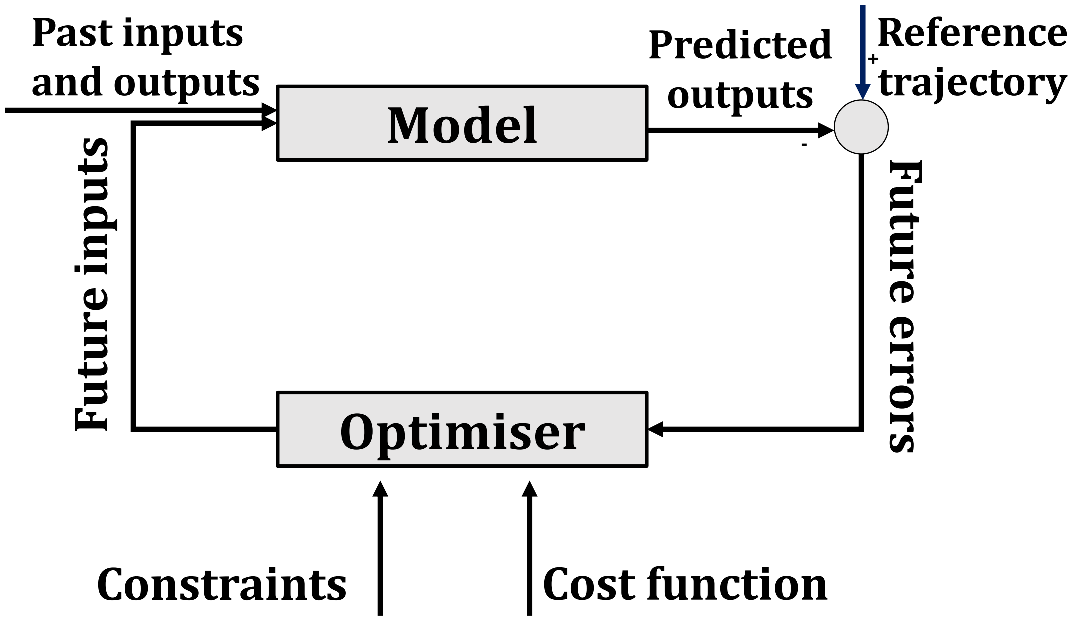

Figure 4: Basic structure of an MPC implementation. (Adapted from Bordons (2000))

design and analysis purposes, they are not tailored for process control. The models used for flotation control are classified and analysed in the following section.

3. Modelling froth flotation for control purposes

Models can be classified in different ways, depending on their characteristics and purposes. For example, Gharai and Venugopal (2016) presented a general classification of the flotation models, identifying two main groups: micro-scale and macro-scale models. Micro-scale models have been used to describe the chemical and physical relationships among sub-processes within a flotation cell (Polat and Chander, 2000; Jovanović et al., 2015). Simplifications and combination of micro-scale models form the basis of macro-scale models, which have been used for the prediction of the behaviour of entire flotation cells – or even banks– the description of process parameters using experimental data, the design of plant layout, and the development of control strategies (Polat and Chander, 2000; Rojas and Cipriano, 2011; Jovanović et al., 2015). Given the massive difference in scale between models for those for an entire cell or banks, it is important to classify models based on both their scale as determining their direct utility for MPC.

Another classification was proposed by Hodouin (2011), who postulated that flotation models can be classified as empirical (used for Principal Component Analysis (PCA), multivariate regression, Partial Least Squares (PLS), neural-networks, transfer functions) or phenomenological; steady-state or dynamic; deterministic or stochastic; causal (input-output model) or non-causal (e.g.: mass conservation constraints); linear or non-linear; based on mathematical equations or fuzzy rules.

In this paper, models are classified into two main groups according to their purpose: models developed for (i) *simulation purposes* (i.e. analysis and design) or (ii) *control purposes*, as shown in Fig. 5. While empirical and phenomenological models can be found for both simulation and control purposes, hybrid models have been developed for control purposes only. Despite the fact that a large number of flotation models have been developed assuming steady-state, these models have been mostly used for design, simulation and off-line optimisation instead of control (Bergh and Yianatos, 2011; Bergh et al., 2013).

It should be noticed, however, that a strict classification of flotation models cannot be proposed, since models can combine aspects of different approaches in order to improve their overall utility (Jovanović et al., 2015). In fact, although there is not a clear distinction between phenomenological and empirical models, the models presented in this paper were classified according to the characteristics that represent them better. The form of empirical models can be influenced by phenomenological considerations, whereas many of the unknown parameters within phenomenological models can be obtained by empirical means. This paper will only focus on froth flotation models for model-based controllers. Reviews on flotation modelling for simulation purposes rather than control can be found in Varbanov et al. (1993); Herbst and Harris (2007); Alves dos Santos et al. (2014); Jovanović et al. (2015); Wang et al. (2015); Gharai and Venugopal (2016); Dinariev and Evseev (2018); Prakash et al. (2018); Wang et al. (2018), among others.

Modelling for control purposes is a difficult task since most of the models developed so

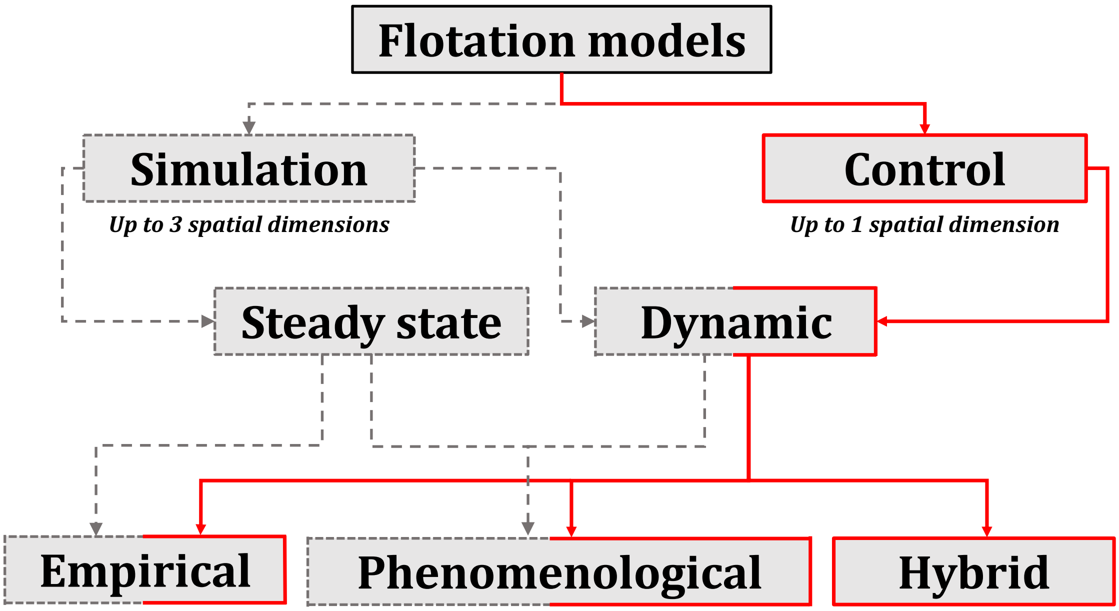

Figure 5: Classification of flotation models according to their final purpose. Flotation models for control purposes must be dynamic, and can be sub-classified as empirical, phenomenological and hybrid (highlighted in solid red lines).

far have physical parameters that cannot be adequately measured (or even estimated) in a plant. Additionally, the complexity of flotation is due to its stochastic behaviour as well as the lack of reliable instrumentation, which makes it more difficult to develop simple models for control purposes that can be calibrated with either industrial (Perez-Correa et al., 1998; Casali et al., 2002; Maldonado et al., 2007b; Putz and Cipriano, 2015) or laboratory-scale (Bascur, 1982; Maldonado et al., 2007a, 2009, 2010; Shean et al., 2017, 2018) data.

It should also be noted that most of the models that have been developed for flotation control have focused on the pulp phase. Simplification of the froth phase (or even completely neglecting it) has been the approach of several authors for flotation process simulations (Bergh et al., 2013). A deeper discussion of the models used for MPC in froth flotation is presented in the following sections. A summary of the models used to represent the each flotation variables mentioned in this literature review manuscript is presented in Table 2.

Table 2: Summary of models of equations used to represent flotation variables as part of different type of models discussed in this literature survey.

Variable	Equation number		
	Empirical model	**Phenomenological model**	**Hybrid model**
Attached particles in the froth phase		(81)	
Attached particles in the pulp phase		(79)	
Attachment rate constant in the froth phase	(27)		
Attachment rate constant in the pulp phase	(23)		
Bias rate	(21)		
bubble surface area flux		(17)	
Bulk fluid velocity due to drainage	(30)		
Collection rate constant	(6)		
Concentrate grade	(12)		
Detachment rate constant in the froth	(29)		
Detachment rate constant in the pulp	(28)		
Drainage rate constant	(4), (7)		
Flotation rate constant	(3), (5)	(34), (35)	
Gas hold-up	(20)	(72), (74)	
Impeller power	(26)		
Liquid holdup	(22)		
Pulp level		(39), (42), (65), (66), (67)	(70)
Sauter mean bubble diameter	(19)	(18)	
Solid mass concentrate flowrate	(10)		
Solid mass in the froth phase		(46), (48), (50), (51)	
Solid mass in the pulp phase		(37), (38), (40), (45), (47), (49), (53), (54)	
Solid mass in the tailings		(43)	
Tailings flowrate	(16)	(41)	
Tailings grade		(44)	
Turbulent aggregate velocity	(24)		
Unattached particles in the froth phase		(80)	
Unattached particles in the pulp phase		(78)	
Upward gas velocity of the bubble in the pulp		(75)	
Volume of liquid in the froth		(69)	
Volume of liquid in the pulp		(68)	
Volumetric concentrate flowrate	(9)		(15)
Water drainage	(32)		
Water entrainment	(31)		
Water in the concentrate	(33)	(58)	

3.1. Empirical models

Empirical models are developed from data analysis through statistical methods that relate input-output measurements from the plant (Shean and Cilliers, 2011). Multiple linear regression methods or spline regression methods are commonly used for such analysis (Mular, 1972; Whiten, 1972; Lynch et al., 1981), from which parameters with limited physical meaning are obtained (Polat and Chander, 2000).

The collection of data for the development of empirical models can be done via online or off-line methods. Online data is obtained via online instrumentation that allows updating the empirical parameters in the model. Off-line collection methods can be based on either daily operating data or from a previously planned campaign (Lynch et al., 1981).

Shorter model development time in comparison with other types of models is one of the main advantages of empirical models, specially when the final purpose of the model that is being developed is previously known. These models are, however, valid only under a certain range of operating conditions and must be used for a particular plant, which treats a particular type of ore, under a well-known operating range. Purely empirical models typically decrease in accuracy rapidly if the conditions move outside the calibration range. Although empirical flotation models have been proposed since the late 60s by Faulkner (1966), Pitt (1968) and Smith and Lewis (1969), these need to be adjusted for each new mineralogical conditions and plant layout to which they are to be applied.

An example of an empirical model used for flotation control is the one developed by Perez-Correa et al. (1998). Flotation kinetics (K_p) and drainage constants (K_e) were empirically determined, by relating them to the effect of collector and frother addition rates. As a result, polynomial relationships (Eqs.(3) and (4)) between these variables were obtained as follows:

$$K_p^i = a_1^i Q_{col}^3 + a_2^i Q_{col}^2 + a_3^i Q_{col} + \kappa_{col,0}^i, \tag{3}$$

$$K_e^i = \kappa_{e0}^i + b_1^i Q_{col} + b_2^i Q_f, \tag{4}$$

where Q_{col} is the collector addition rate, and Q_f is the frother addition rate. The empirical parameters (a_1, a_2, a_3, $\kappa_{col,0}$, κ_{e0}, b_1 and b_2) were determined for each mineralogical class. In the study by Perez-Correa et al. (1998), the mineralogical classes considered were (1) "rich mineral", mainly chalcopyrite, and (2) "poor mineral", mainly gangue. Since experimental data showed that the amount of iron in the poor classes in the feed stream directly affected the rougher concentrate grade, the flotation rate constant of the poorest mineralogical class was instead represented by the Eq.(5). A more comprehensive study would include more mineralogical classes as the iron can be present in more than one mineral or as mixed mineral grains, which would further complicate the model of the flotation rate constant.

$$K_{pf}^{i} = \kappa_{p}^{i} \left(1 + 0.1 \left(g_{Fe} - g_{Fe,0}\right)\right), \tag{5}$$

where K_{pf}^{i} is the flotation rate of the poorest mineralogical class modified by iron content, κ_{p}^{i} is the flotation rate of mineralogical class i from Eq.(3), g_{Fe} is the iron grade, and $g_{Fe,0}$ is the initial iron grade. It should be noted that this flotation rate model is rather unconventional, and it was not found in any other study analysed in this literature survey.

Interestingly, despite the fact that the frother and collector flowrates were originally defined as manipulated variables by Perez-Correa et al. (1998), these variables were in the end considered as disturbances in three of the four simulated cases, and only the pulp level was considered as a manipulated variable when implementing the control strategies. Additionally, the accuracy of the models was not reported as the focus of the study was to compare different control strategies rather than to develop and test control models.

While the models for the above mentioned kinetic constants (i.e. Eqs.(3) and (4)) were developed for different mineralogical classes i, Putz and Cipriano (2015) extended these models to consider not only a change in each mineralogical class, but also in each cell j, and for each granulometry class k, as shown in Eqs.(6) and (7). Neither Perez-Correa et al. (1998) nor Putz and Cipriano (2015) reported the value of any of the adjustable parameters in the models.

$$K_{col}^{ijk} = a_{1}^{ijk} Q_{col}^{3} + a_{2}^{ijk} Q_{col}^{2} + a_{3}^{ijk} Q_{col} + \kappa_{col,0}^{ijk}, \tag{6}$$

$$K_e^{ijk} = b_1^{ijk} Q_{col} + b_2^{ijk} Q_f + \kappa_{e0}^{ijk}, \tag{7}$$

where K_{col}^{ijk} is the collection rate constant, and K_e^{ijk} is the drainage constant. Flotation rate constants were also modelled by Maldonado et al. (2007a), for a rougher flotation control strategy based on dynamic programming (Bertsekas, 1995). In their implementation, both phenomenological and empirical models were used. The phenomenological models from their work can be found in Section 3.2, Eqs.(40) to (44). For their empirical models, flotation rate constants (K_{ij}) for each mineralogical class i in the flotation bank j, were estimated as a function of froth depth (h_f), tailings grade (g_T), tailings volumetric flowrate (Q_T) and empirical parameters (p), as shown in Eq.(8). Several sampling tests in a Chilean mine were conducted to validate the proposed models, with the model parameters determined by using the standard least squares algorithm.

$$K_{ij} = f\left(h_{f_j}, g_{T_{i(j-1)}}, Q_{T_{j-1}}, p\right). \tag{8}$$

The concentrate volumetric flowrate (Q_C) was calculated as a linear function of froth height (h_f), as shown in Eq.(9).

$$Q_{C_j} = c_{1j} - c_{2j} h_{f_j}, \tag{9}$$

where c_{1j} and c_{2j} are empirical parameters.

Even predominantly empirical models can be influenced in their form by phenomenological considerations, as in Eq.(10), in which the concentrate mass flowrate ($M_{SC_{ij}}$) depends on the empirical flotation constant (K_{ij}, from Eq.(8)). The concentrate mass flowrate was used to calculate the total solid mass flowrate (M_{SC}, from Eq.(11)) and concentrate grade ($g_{C_{ij}}$, from Eq.(12)) as follows:

$$M_{\mathrm{SC}_{ij}} = K_{ij} M_{\mathrm{SP}_{ij}}, \tag{10}$$

$$M_{\mathrm{SC}_j} = \sum_{i=1}^{3} M_{\mathrm{SC}_{ij}}, \tag{11}$$

$$g_{C_{ij}} = 100\frac{M_{\mathrm{SC}_{ij}}}{\sum_{k=1}^{3} M_{\mathrm{SC}_{kj}}}, \tag{12}$$

where $M_{SP_{ij}}$ is the solid mass in the slurry, while the cumulative concentrate solid ($M_{SC_{ij}}$) mass flowrate was defined as shown in Eq.(13):

$$M_{\mathrm{SCC_j}} = \sum_{k=1}^{j} M_{\mathrm{SC_k}}, \tag{13}$$

and the cumulative concentrate grade (g_{CC_j}) was defined as:

$$g_{\mathrm{CC}_j} = 100\frac{\sum_{k=1}^{j} M_{\mathrm{SC}_{1k}}}{\sum_{k=1}^{j}\sum_{i=1}^{3} M_{\mathrm{SC}_{ik}}}. \tag{14}$$

Regarding the estimation of concentrate volumetric flowrate, Putz and Cipriano (2015) also presented a model that does not only depend on the froth height, but also on the pulp level, feed and tailings volumetric flowrate, and logic rules [1] (δ_1 and δ_2), as shown in Eqs.(15) and (16):

$$\mathrm{Q}_C^i = \alpha_C^i \left(h_P^i + h_F^i - h_{\max}^i\right) \delta_1^i \delta_2^i + \left(\mathrm{Q}_F^i - \mathrm{Q}_T^i\right)\left(1 - \delta_1^i\right), \tag{15}$$

where α_C^i is a tuning constant, h_P is the pulp level, h_f is the froth height, and h_{max} is the total flotation cell height. It is important to note that the froth height was considered constant due to an absence of advanced models to estimate it.

$$Q_T^i = \alpha_T^i u_i \sqrt{h_P^i - h_P^{i+1} + \Delta h^i}, \tag{16}$$

where α_T^i is a tuning constant, u_i is the control valve position, and Δh is the physical height difference of two consecutive flotation cells. It should be noted that there is usually a minor difference in height between cells, but a significant difference in pulp level between cells as the mass is removed down a flotation bank. This model is based on Torricelli's principle and depends on the position of the output control valve ($u_i \in \{0, 1\}$). The Torricelli's principle relates the velocity of fluid leaving a cylinder (as the flotation tank) to the height of the fluid.

[1] Logic rules are part of hybrid models, which are addressed in Sec. 3.3.

In this context, Torricelli's principle was used to develop a model for the tailings flowrate in terms of the pulp height (or "fluid height") and the control valve.

A nonlinear controller for the bubble surface area flux was designed by Maldonado et al. (2010). The controlled variable was the bubble Sauter diameter and the manipulated variable was the superficial water velocity that passes through a sparger ring that was installed in the experimental rig, which allowed to control the bubble size independently from gas velocity. The sparger ring used was a "frit-and-sleeve" sparger, specially designed by Kracht et al. (2008), which uses a porous ring and a sleeve to control the bubble size, as described in Maldonado et al. (2010). The bubble surface area flux (S_b) can be calculated as Eq.(17), and it can be controlled by manipulating the ratio between superficial gas velocity (J_g) and the Sauter mean bubble diameter (d_{32}):

$$S_b = \frac{6J_g}{d_{32}}, \tag{17}$$

where d_{32} is calculated as:

$$d_{32} = \frac{\sum_{i=1}^{N_b} d_{BP_i}^3}{\sum_{i=1}^{N_b} d_{BP_i}^2}, \tag{18}$$

where d_{BP} is the bubble diameter in the pulp phase, and N_b is the number of bubble size classes.

As can be seen, Eqs.(17) and (18) are not explicitly time dependant, and therefore, an online estimation of the Sauter mean bubble diameter, previously proposed by Maldonado et al. (2008), was implemented. A nonlinear steady-state relationship between Sauter mean diameter (d_{32}), and superficial water velocity (J_{ls}) was obtained, as shown in Eq.(19).

$$d_{32} = 3.706 \cdot J_{ls}^{-0.256} - 0.226. \tag{19}$$

The strong influence of frother concentration on bubble size was also subject of flotation control research by Maldonado (2010), who considered frother concentration as an unmeasured disturbance that directly affects flotation performance due to its impact on bubble size and froth stability. Maldonado et al. (2009) used electrical conductivity to calculate the gas hold-up (ε_g) in a laboratory scale flotation column, as shown in Eq.(20). Froth height was also considered constant for the dynamic models used to implement the control strategy.

$$\varepsilon_{\mathrm{g}} = 100\left(\frac{k_l - k_{l-g}}{k_l + 0.5k_{l-g}}\right), \tag{20}$$

where k_l and k_{l-g} are the conductivity for the liquid and liquid-gas mixture, respectively.

The constrained controller implemented in Maldonado et al. (2009) was used to minimise the tracking error of the gas hold-up (ε_g) and bias rate (J_B), which is defined as the net downward water flowrate (i.e. bias rate = tailings flowrate (water) - feed flowrate (water)) (Del Villar et al., 1999). The bias rate (J_B) was calculated through the empirical equation shown in Eq.(21), as a function of the fraction of wash water, which is also calculated by using conductivity (Eq.(22)). In flotation columns, wash-water rate (J_w) is a crucial operating variable as it is directly linked to froth stability and it is used to enhance drainage, thus reducing entrainment. This is an important variable to control in flotation columns since a very high wash-water rate can lead to inefficient froth cleaning action due to increasing in froth mixing and water short-circuiting to the concentrate, limiting the overall metallurgical performance (Yianatos and Bergh, 1995). Table 3 shows the six inequality equations that were implemented by Maldonado et al. (2009).

$$J_{\mathrm{B}} = 0.003966 \cdot \varepsilon_{\mathrm{w}} - 0.03409, \tag{21}$$

The liquid hold-up (ε_w) is calculated as:

$$\varepsilon_{\mathrm{w}} = 100\left(\frac{k_{\mathrm{f}} - k^*}{k_{\mathrm{f}} - k_{\mathrm{w}}}\right), \tag{22}$$

where k_f is the conductivity of the water in the feed, k^* is the conductivity of the interface, and k_w is the conductivity of wash-water.

Although the use of sensors based on conductivity was not of major concern to Maldonado et al. (2009) since these sensors have been satisfactorily tested on plants (Gomez et al., 2003; Bartolacci et al., 2008), differences in the estimation of bias rate were found when comparing these measurements to a water balance in the collection zone. This suggests that

Table 3: Description of operational constraints proposed by Maldonado et al. (2009)

Constraint	Description
$J_g \leq J_{g_{\max}}$	To prevent: hydraulic entrainment, loss of the interface and froth "burping"
$J_g \geq J_{g_{\min}}$	To keep solid in suspension
$J_{\mathrm{w}} \leq J_{\mathrm{w}_{\max}}$	To avoid: froth mixing and wash-water short circuiting
$J_{\mathrm{w}} \geq J_{\mathrm{w}_{\min}}$	To promote froth stability and to facilitate transfer of collected particles into the concentrate
$J_{\mathrm{B}} \leq J_{\mathrm{B}_{\max}}$	To avoid reduction of collection residence time for valuable minerals
$J_{\mathrm{B}} \geq J_{\mathrm{B}_{\min}}$	To perform cleaning action thus reducing gangue entrainment

either the conductivity measurements have an intrinsic error that should be considered when controlling a flotation column using the proposed models, or that the model relating liquid hold-up to flowrate is the source of the error.

The fact that froth height has been assumed constant in most models for flotation control indicates there is an opportunity to enhance these models so that they also take into account all the phenomena that occur in the froth phase. For example, particle attachment and detachment processes in the froth phase have been considered in some studies, such as Zaragoza and Herbst (1989), in which a hierarchical control based on a simplified version of the models proposed by Bascur (1982) was implemented. In order to simplify those models, Zaragoza and Herbst (1989) assumed that the attachment and detachment processes are at equilibrium in the pulp and the froth phases. This assumption is questionable in terms of application for control since this equilibrium may be affected by dynamic changes in, for example, particle size, head grade in the feed, and particle liberation.

The rate constants of the attachment phenomena in the pulp phase (K_{ij}^{PAT}), can be modelled as shown in Eq.(23) (Bascur, 1982):

$$K_{ij}^{PAT} = \kappa_j^{PAT} \frac{v_{BP} d_{iB}^2 u_t}{d_{BP}^3}, \tag{23}$$

where κ_j^{PAT} is a constant which is determined experimentally, v_{BP} is the volume of bubbles in the pulp phase, d_{iB} is the mean size of the aggregate particle-bubble of size i, and d_{BP} is the bubble diameter in the pulp phase. The turbulent aggregate velocity (u_t) can be estimated using Eq.(24) (Schubert, 2008):

$$\sqrt{\Delta v_{\mathrm{t}}'^2} \approx 0.33 \frac{\varepsilon^{4/9} d_{\mathrm{p}}^{7/9}}{v_{\mathrm{F}}^{1/3}} \left(\frac{\Delta\rho}{\rho_{\mathrm{F}}} \right)^{2/3}. \tag{24}$$

where ϵ is the average energy dissipation, d_p is the particle size, v_F is the kinematic fluid viscosity, $\Delta\rho$ is the density difference between particle and fluid, and ρ_F is the fluid density.

The average energy dissipation (ϵ) in a flotation tank is given by Eq.(25):

$$\epsilon = \frac{P_g}{V_{LP}}, \tag{25}$$

where P_g is the power drawn by the impeller, and V_{LP} is the volume of liquid in the pulp. The power drawn by the impeller can be obtained from dimensional analysis, as in Eq.(26):

$$\frac{P_g}{P_0} = e_1 \left(\frac{Q_A}{N_I D_I}\right)^{e_2} \left(\frac{N_I^2 D_I^3 \rho_L}{\sigma}\right)^{e_3}, \tag{26}$$

where P_0 is the power input to impeller when no air is added, D_I is the impeller diameter and N_I is its speed, Q_A is the air flowrate, ρ_l is the density of water and σ is the surface tension. e_1, e_2 and e_3 are constants.

The rate constant of the attachment process in the froth phase (K_{ij}^{FAT}) is modelled as shown in Eq.(27). This model is a function of collision frequency ($\frac{d_P}{d_{BF}}$), and the number of bubbles across the height of the froth (Bascur, 1982).

$$K_{ij}^{FAT} = \kappa_j^{FAT} Q_A \left(\frac{d_p}{d_{BF}}\right) \left(\frac{h_f}{d_{BF}}\right), \tag{27}$$

where κ_j^{FAT} a constant which is determined experimentally, Q_A is the volumetric air flowrate in the pulp, d_p is the particle size, d_{BF} is the bubble size in the froth, and h_f is the froth height.

The constants rate of detachment phenomena in both pulp and froth phases were also determined by empirical equations. In the pulp phase, the rate of detachment (K_{ij}^{PDT}) is given by Eq.(28).

$$K_{ij}^{PDT} = \kappa_j^{PDT} d_P^2 u_t, \tag{28}$$

where d_p is the particle size and u_t is the turbulent velocity that can be calculated as Eq.(24). In the froth phase, the rate constant of detachment (K_{ij}^{FDT}) is given by Eq.(29):

$$K_{ij}^{FDT} = \kappa_j^{FDT} \rho_j d_P^n u_\infty, \tag{29}$$

where ρ_j represents the specific gravity of species j, n is an adjustable constant, and u_∞ is the bulk fluid velocity due to drainage, which can be approximated by Eq.(30):

$$u_\infty = \frac{Q_R}{A_3(1-\varepsilon_g)}, \tag{30}$$

where Q_R represents the volumetric drainage rate and $A_3(1-\varepsilon_g)$ represents the effective cross sectional area of the liquid phase in the froth.

The population balance approach needs to be complemented with hydraulic models as the liquid distribution between the pulp and froth is required. For this, Bascur (1982) proposed empirical models that allow the estimation of water entrainment (Q_E), water drainage (Q_R) and water reporting to the concentrate (Q_C), which can be calculated by Eqs.(31), (32) and (33), respectively.

$$Q_E = a_4 \frac{Q_A}{d_{BP}^{0.75}}, \tag{31}$$

$$Q_R = a_5 \frac{\left(\frac{Q_A}{A}\right)^{0.53} V_{LF}^{0.56} A^{0.4}}{\sigma^{0.24} d_{BF}^{1.92}}, \tag{32}$$

$$Q_C = a_6 L \left(h_f - h_{max}\right)^{1.5} \left(1-\varepsilon_g\right), \tag{33}$$

where a_4, a_5 and a_6 are adjustable parameters, L is the overflowing lip length of the cell, h_f is the froth height, h_{max} is the total flotation cell height, σ is the surface tension, A is the cross-sectional area of the froth volume, and ε_g is the gas hold-up. Plant data were used in order to estimate the parameters required in the aforementioned equations (Bascur, 1982; Zaragoza and Herbst, 1989).

One major drawback of empirical models is that they are no useful for operating conditions other than those used to develop the model. The operating conditions in an industrial process, however, usually change, resulting in empirical models having limited accuracy and robustness. In particular for the flotation process, changes in feed mineralogy, particle size, reagents, among many other variables, are common and have a large impact in the operation at industrial scale, and should therefore be considered when modelling for control.

One solution to these model mismatches is the development of phenomenological models for control. Phenomenological models are based on fundamental aspects of the process (e.g. physics or surface chemistry), and are able to predict changes in operating conditions, achieving the robustness necessary to be applied in MPC strategies without the need for significant additional model development. Phenomenological models for flotation control are the focus on the next section.

3.2. Phenomenological models

Unlike empirical models, a phenomenological model is derived from fundamental laws. While phenomenological models for simulation or analysis purposes have often been subclassified as kinetic, population balance and probabilistic (Polat and Chander, 2000; Gharai and Venugopal, 2016), the latter are not found in the literature pertaining to flotation predictive control. In this paper, instead, models are classified as kinetic, population balance, and hydraulic, all of which are discussed below.

It must be taken into account that while several phenomenological flotation models already exist, most of them have been used for design or analysis purposes since they are often not simple enough to be implemented into control strategies. Additionally, models for design and analysis purposes can be steady-state, whereas MPC requires dynamic models.

3.2.1. Kinetic models

Kinetic models are developed by considering processes as analogous to a chemical reaction. Lynch et al. (1981) described this "reaction" in flotation by considering two types of collisions: (i) between molecules and (ii) between hydrophobic particles and air bubbles in the pulp. Simple kinetic descriptions, however, may ignore the contribution of the froth to the overall transport of both the valuable material and the gangue. These kinetic descriptions can therefore be extended to include the transfer of material not just out of the pulp phase, but also into and out of the froth phase. A schematic of particles transfer from pulp to froth or vice-versa is shown in Fig. 6. This schematic represents particle transfer from the pulp phase due to selective attachment or non-selective entrainment, as well as the particle transfer from the froth phase to the pulp phase due to drainage.

By considering flotation as a chemical reaction, a kinetics model can be derived, as shown in Eq.(34) (Garcia-Zuniga, 1935; Arbiter and Harris, 1962; Gharai and Venugopal, 2016).

$$\frac{dN}{dt} = -K_n N^n N_b^m, \tag{34}$$

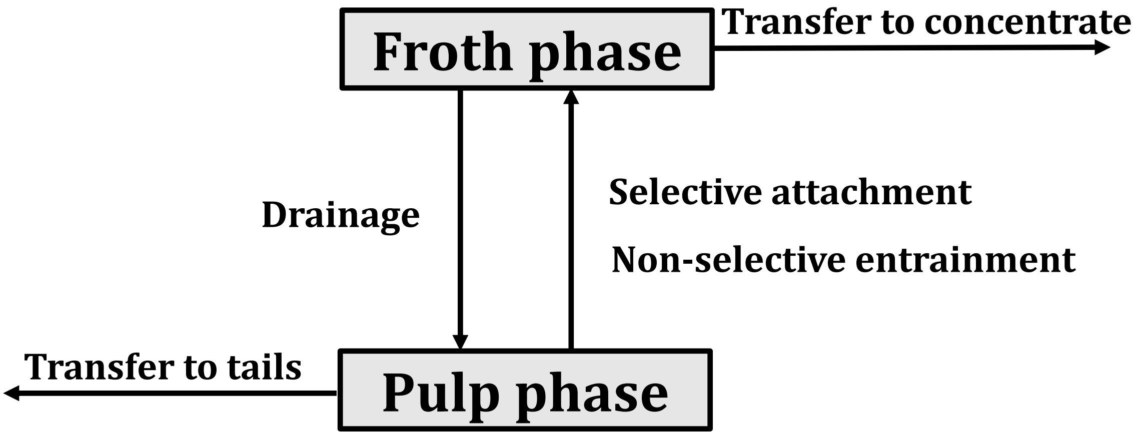

Figure 6: Transfer of material between pulp and froth regions in a flotation process (Adapted from Lynch et al. (1981))

where K is the flotation rate constant, N is particle concentration, N_b is the bubble concentration; n and m are their respective kinetic orders. The negative sign is due to the fact that concentration decreases as particles leave the flotation cell.

Generally, flotation kinetics are considered to be first-order (Gharai and Venugopal, 2016), as shown in Eq.(35) (Kelsall, 1961; Arbiter and Harris, 1962; Yoon and Mao, 1996)), with the bubble concentration dependency absorbed into the rate constant:

$$\frac{dN}{dt} = -KN. \tag{35}$$

Nguyen et al. (1998) developed a first order kinetics model considering three-components according to their floatability: non-floating, slow and fast, as shown in Eq.(36):

$$Rec = 1 - m_f \exp\left(-K_f t\right) - m_s \exp\left(-K_s t\right) - m_{\mathrm{n}}, \tag{36}$$

where m_n, m_s and m_f are the mass fractions of non-floating, slow and fast floating species, respectively; and K_f and K_s are the respective flotation rate constants. More recently, Neethling et al. (2019) have shown that flotation cells can sometimes experience zero-order kinetics, and explored the cases when this can happen, carrying out modelling and validation. In order to model the transition between first and zero order kinetics, assuming that the cell is well mixed, the "reaction" is considered to be between the particles and the available bubble surface area flux, the flotation rate was defined as Eq.(37):

$$M_i = K_i C_{p,i} \varepsilon_g \chi_b \left(1 - \frac{\varepsilon_g}{\varepsilon_{g,\max}}\right) V_{cell}, \tag{37}$$

where M_i is the solid mass of the specie i, K_i is the flotation rate constant, $C_{p,i}$ is the solid concentration, ε_g is the gas hold-up, χ_b is the bubble surface area, and V_{cell} is the cell volume.

Although this approach that accounts for this transition kinetics has not been implemented into any control strategy yet, it is amenable to be tested in future studies. Even though numerous kinetic models have been developed for froth flotation analysis and design, as discussed in Gharai and Venugopal (2016) and Mesa and Brito-Parada (2019), it is worth mentioning only those kinetic models used for control purposes are discussed within this section. Therefore, some of the key aspects of kinetic models – such as K distribution, for example – are not discussed in this paper.

In terms of flotation control, a study on the optimal control of a rougher flotation circuit can be found in Maldonado et al. (2007a), based on a dynamic simulator developed by Casali et al. (2002). The models developed by Casali et al. (2002) are shown in equations 38 and 39. Mass balance models for the pulp phase of a nine-cells rougher flotation circuit of sulphide copper ore were implemented, assuming five mineral classes, perfect mixing, and constant air flowrate.

$$\frac{\mathrm{d}M_{ij}}{\mathrm{d}t} = -\left[K_{ij} + \frac{Q_{\mathrm{Tj}}}{(1-\varepsilon_{\mathrm{g}})\,AN_j}\right] M_{ij} + M_{\mathrm{S}_{ij}}, \quad i = 1, \ldots, 5 j = 1, \ldots, 9, \tag{38}$$

where M_{ij} is the solid mass of the specie i of the cell j, K_{ij} is the flotation rate constants, Q_{Tj} is the tailings volumetric flowrate in the cell j, ε_g is the gas hold-up, A is the cross-sectional area of the cell, N_j is the particle concentration in the cell j, and $M_{S_{ij}}$ is the solid mass flowrate. The pulp level h_P of the cell j is calculated by Eq.(39:

$$\frac{\mathrm{d}h_{P_j}}{\mathrm{d}t} = \frac{Q_{\mathrm{F}_j} - Q_{\mathrm{C}_j} - Q_{\mathrm{T_j}}}{(1-\varepsilon_{\mathrm{g}})\, A}, \quad j = 1, \ldots, 9, \tag{39}$$

where Q_{Fj} is the feed volumetric flowrate to the cell j, Q_{Cj} is the concentrate volumetric flowrate from the cell j, and Q_{Tj} is the tailings volumetric flowrate from the cell j.

Similarly to Casali et al. (2002), Maldonado et al. (2007b) implemented mass balance models for the pulp phase, but only three mineralogical classes and five flotation cells were considered. The solid mass in the pulp was calculated using the Eq.(40), while Eq.(41) was used to describe the tailings volumetric flowrate. It must be noticed that the tailings volumetric flowrate can also be calculated empirically, as previously shown in Eq.(7). The models included the time variation for each mineralogical class i in cell j of the solid mass M_{ij} in the pulp phase, and the pulp level h_{p_j} in each cell.

$$M_{\mathrm{SP}_{ij}} = \frac{M_{\mathrm{ST}_{j-1}} g_{T_{i(j-1)}}}{\left(\tilde{k}_{ij} + \frac{Q_{T_j}}{Ah_{p_j}}\right)}, \tag{40}$$

where $M_{ST_{j-1}}$ is the solid mass flowrate in the tailings, $g_{T_{i(j-1)}}$ is the metallurgical grade in the tailings.

$$Q_{T_j} = Q_{T_{j-1}} - Q_{C_j}, \tag{41}$$

Froth depth, tailings solid mass flowrate and tailings grade were also implemented into the MPC strategy tested by Maldonado et al. (2007a), by using phenomenological models as follows:

- The froth depth (h_{fj}) for each cell was calculated as the difference between the cell total height (H) and pulp level (h_{p_j}), as shown in Eq.(42):

$$h_{f_j} = \left(H - h_{p_j}\right) \cdot 1000(mm). \tag{42}$$

- The tailings solid mass flowrate for each mineralogical class i in the bank j ($M_{ST_{ij}}$) was calculated using the Eq.(43):

$$M_{\mathrm{ST}_{ij}} = \frac{Q_{T_j}}{Ah_{p_j}} M_{\mathrm{SP}_{ij}}, \tag{43}$$

  where $M_{SP_{ij}}$ is the solid mass in the pulp phase.

- The tailings grade for each mineralogical class i in the flotation bank j ($g_{T_{ij}}$) was calculated by assuming perfect mixing in the flotation cells, using the Eq.(44):

$$g_{T_{ij}} = 100 \frac{M_{\mathrm{SP}_{ij}}}{\sum_{k=1}^{3} M_{\mathrm{SP}_{kj}}}. \tag{44}$$

In the same study (Maldonado et al. (2007b)) empirical models were also implemented, as was previously shown in Eqs.(8) to (14) (Section 3.1). While Casali et al. (2002) and Maldonado et al. (2007b) have considered the effect of gas hold-up (ε_g) in their mass balances (Eqs.(38) and (39)), Putz and Cipriano (2015) developed mass balances that considered the attachment and detachment processes rather than gas hold-up, as shown in Eqs.(45) and (46). In this case, i represents the cell number of the bank, j represents the mineral class (defined as high or low) and k represents the different granulometries in the ore.

$$\frac{dM_p^{ijk}}{dt} = M_f^{ijk} + K_e^{ijk} M_f^{ijk} - \left[K_P^{ijk} + \frac{Q_T^i}{V_P^i}\right] M_P^{ijk}, \tag{45}$$

$$\frac{dM_f^{ijk}}{dt} = K_P^{ijk} M_P^{ijk} - \left[K_e^{ijk} + \frac{Q_C^i}{V_F^i}\right] M_f^{ijk}, \tag{46}$$

where M_p^{ijk} is the mass of solids in the pulp phase and M_f^{ijk} is the mass of solids in the froth phase. K_e^{ijk} and K_p^{ijk} are the respective flotation rates constants, Q_T is the tailings flowrate from the cell i, V_P^i and V_F^i are the pulp and froth volume of the cell i, respectively. The collection and drainage rate were determined empirically, as shown previously in Eqs.(6) and (7).

Another kinetic balance approach that considers the attachment and detachment processes is that in Zaragoza and Herbst (1989). In this work, simplified models for the pulp (Eq.(47)) and froth phase (Eq.(48)) were proposed in order to implement an advanced model-based control in a 2-cells flotation circuit.

$$
\begin{aligned}
\frac{dM_p}{dt} =& M_{FD} - \left(Q_T + Q_E + Q_A \frac{1-\varepsilon_g}{\varepsilon_g} \alpha^p \right) \\
& \cdot \frac{M_p}{\left(1+\alpha_p\right) V_{LP}} + \frac{K_R Q_R}{V_{LF}} \cdot \frac{M_f}{\left(1+\alpha_f\right)},
\end{aligned} \tag{47}
$$

$$
\begin{aligned}
\frac{dM_f}{dt} =& -\left(Q_R K_R + Q_c \left(1+\alpha_f\right)\right) \frac{M_f}{\left(1+\alpha_f\right) V_{LF}} \\
& + \left(Q_T + Q_A \frac{1-\varepsilon_g}{\varepsilon_g} \alpha_p \right) \frac{M_p}{\left(1+\alpha_p\right) V_{LP}},
\end{aligned} \tag{48}
$$

where M_p and M_f are the solid mass in the pulp and froth, respectively. M_{FD} is the mass flowrate in the feed, Q_T is the tailings flowrate, Q_E is the entrainment water flowrate, Q_A is the air flowrate, ε_g is the gas hold-up, α_p and α_f are the equilibrium constant between the attachment and detachment in the pulp and froth phases, respectively. V_{LP} is the volume of the liquid in the pulp, V_{LF} is the volume of the liquid in the froth, and Q_R is the water flowrate draining back.

These models were also coupled with an overall volume balance in the flotation cells, as shown in Eq.(68) and Eq.(69), in the next section. Another similar approach, i.e. considering attachment and detachment processes in the pulp and froth phases, was proposed by Tian et al. (2018), where dynamic models were implemented into the model predictive control strategy for a 2-phase flotation column. These models have one spatial dimension in addition to the temporal dimension for which they were also solved. The pulp and froth phases were modelled via mass balances, considering the mass concentration of solid particles (free mineral, locked and gangue) within the "air phase" and "water phase". Ordinary differential equations (ODEs) were used to model the solid particles in the pulp phase, as shown in

Eqs.(49) and (50):

$$\frac{d\left(\varepsilon_g V C_a(t)\right)}{dt} = \alpha_1 A v f \varepsilon_w V C_w(t) - \beta \varepsilon_g V C_a(t) - Q_A C_a(t), \tag{49}$$

$$\begin{aligned}\frac{d\left(\varepsilon_w V C_w(t)\right)}{dt} &= -\alpha_1 A v f \varepsilon_w V C_w(t) + \beta \varepsilon_g V C_a(t) \\ &+ Q_F C_F - Q_T C_w(t) + Q_{w_d} C_{w_d}(0,t) - Q_{w_u} C_w(t),\end{aligned} \tag{50}$$

where ε_g is the gas hold-up, V is the volume of the pulp phase in a flotation column, C_a, C_w, C_{w_d}, C_{w_u} are the mass concentration of solid particles in the air phase, water phase, downward water phase, and upward water phase, respectively. α_1 is the attachment rate constant and β is the detachment rate parameter, A_v is the air-water interfacial area per unit volume of the flotation column, f is the fractional free surface area of the bubbles, ε_w is the hold-up of the water phase, Q_A is the air flowrate, Q_F is the feed flowrate, Q_T is the tailings flowrate, Q_{w_u} is the upward water flowrate, and Q_{w_d} is the downward water flowrate.

The froth phase was modelled by using Partial Differential Equations (PDEs), considering the froth as a Plug Flow Reactor (PFR). The PFR assumption considers that the froth phase is not mixed in the flow direction, but is perfectly mixed in the direction perpendicular to the flow. However, it should be noted that modelling the pulp as a plug flow reactor is only applicable to a column cell and, even there, it ignores the substantial vertical mixing which may occur in these systems. The solid mass balance for the air phase was modelled as shown in Eq.(51):

$$\begin{aligned}\frac{\partial\left(\varepsilon_g C_a^F(z,t)\right)}{\partial t} &= -\frac{\partial\left(U_a C_a^F(z,t)\right)}{\partial z} \\ +\alpha_1 A v f C_{w_d}(z,t) &+ \sigma_1 A v f C_{w_u}(z,t) - \beta C_a^F(z,t),\end{aligned} \tag{51}$$

where U_a is the velocity of particles within the air phase. The term $\alpha A_v f C_{w_d}$ represents the transfer of particles from the downward water flow to the bubble; the term $\sigma_1 A_v f C_{w_u}$ represents the transfer of particles from the upward water flow to the babble; and the term βC_a^F represents the particles detachment from the bubble.

The initial conditions for the collection zone models used by Tian et al. (2018) were:

$$C_a(0) = C_{a0}, \quad C_w(0) = C_{w0}, \tag{52}$$

while for the pulp phase, two cases were considered: downward water motion and upward water motion, as shown in Eqs.(53) and (54), respectively:

$$\begin{aligned} \frac{\partial\left(\varepsilon_{w_d} C_{w_d}(z,t)\right)}{\partial t} &= \frac{\partial\left[\left(U_{w_d} + \varepsilon_{w_d} U_s\right) C_{w_d}(z,t)\right]}{\partial z} \\ -\alpha_1 A v f C_{w_d}(z,t) &+ \rho_1 C_{w_u}(z,t) + k\beta C_a^F(z,t), \end{aligned} \tag{53}$$

$$\begin{aligned} \frac{\partial\left(\varepsilon_{w_u} C_{w_u}(z,t)\right)}{\partial t} &= -\frac{\partial\left(U_{w_u} C_{w_u}(z,t)\right)}{\partial z} \\ -\sigma_1 A v f C_{w_u}(z,t) - \rho_1 C_{w_u}(z,t) &+ (1-k)\beta C_a^F(z,t), \end{aligned} \tag{54}$$

where the term $\rho_1 C_{w_u}$ represents the transfer of particles from the upward water flow to the downward water flow.

The boundary and initial condition for the PDEs were:

$$C_a^F(0,t) = C_a(t), \quad C_{w_u}(0,t) = C_w(t), \quad C_{w_d}(h,t) = 0, \tag{55}$$

$$C_a^F(z,0) = f_a(z), \quad C_{w_u}(z,0) = f_{w_u}(z), \quad C_{w_d}(z,0) = f_{w_d}(z). \tag{56}$$

A discrete controller was designed by Tian et al. (2018) in order to implement it as part of a flotation column control system. The feed flowrate was used as the manipulated variable while the concentrate grade was used as the controlled variable. Nonetheless, it has to be emphasised that this is not a realistic case scenario as in most flotation cells the feed flowrate is a known disturbance rather than a manipulated variable. To carry out this strategy, the Cayley-Tustin time discretisation transformation (Humaloja and Dubljevic, 2018) was used to discretise the coupled ODE-PDEs. A large number of parameters and variables were considered as constants by Tian et al. (2018) to evaluate their proposed MPC strategy.

Among the variables considered as constants were the height of froth phase and collection region, the air hold-up, air flowrate, attachment and detachment rate parameters (for a full list and the values used for constants, the reader is referred to Table 1 in Tian et al. (2018), although no details were provided for the values given to each parameter or variables). Assuming key variables remain constant is far from optimal, as changes can have a significant impact on operating conditions. For example, while gas hold-up was assumed to be constant in both the pulp and froth phases by Tian et al. (2018), this is a variable that is not only prone to change but also one that is related to pulp height (Shean et al., 2018), as discussed in subsection 3.2.2, and thus has a direct impact on the overall performance of the flotation system. Further work is therefore needed to improve the models, so that the impact of changes in key parameters, such as froth height and gas hold-up, can be predicted.

While Zaragoza and Herbst (1989) also considered attachment and detachment processes in their balances, Tian et al. (2018) developed a model that was not only a function of time but also of space (1-dimensional). Since the latter considered ODEs to represent the pulp phase (only time dependent) and PDEs to represent the froth phase (time and space dependent), Eqs.(49) to (54) were coupled, with the ODE system providing boundary conditions for the PDE system. Although both Zaragoza and Herbst (1989) and Tian et al. (2018) attempted to integrate the phenomenology of the froth phase into control strategies, their approach was based on kinetic models, rather than the physics of the process. While kinetics can represent the pulp phase, the froth phase is significantly more complex, and it is dominated by phenomena such as bubble coalescence and bubble bursting. Kinetic models are not therefore sufficient to fully represent this phase. Enhancement of flotation control can be achieved by including more of the important phenomena involved in the process and, for this reason, including froth physics aspects is essential to develop advanced control strategies.

The dynamic of the flotation froths has a strong influence on the overall performance of flotation cells, and thus, its control is difficult to achieve (Neethling and Brito-Parada, 2018). In addition to those controllers based on froth images (such as those mentioned in the introduction), only a few researchers have addressed the integration of froth performance into control strategies. One example of this is the study carried out by Shean et al. (2017), in which an optimisation system was implemented at laboratory scale, based on the Generating Set Search (GSS) algorithm. This control algorithm was based on maximising the air recovery – a measurement of froth stability – which was developed and validated in a flotation tank at laboratory scale. Air recovery is defined as the fraction of air entering a flotation cell that overflow as unburst bubbles (Neethling and Cilliers, 2008). Air recovery can be calculated at steady-state as:

$$\alpha = \frac{v_f h_f L \eta}{Q_A}, \tag{57}$$

where v_f is the overflowing froth velocity, which is usually measured through image analysis; h_f is the height of the overflowing froth over the lip, L is the lip length, η is the fraction of air in the froth, which is usually close to 1, and Q_A is the air flowrate into the flotation cell.

It has been demonstrated that a peak in air recovery (PAR) is linked to improvements in metallurgical performance (Hadler and Cilliers, 2009; Hadler et al., 2010). For this reason, Shean et al. (2017) considered PAR as the objective in the optimisation problem in order to find the best operating condition (in this study, air flowrate) for the flotation tank. However, it should be noted that this PAR optimisation was only tested for a single flotation tank, which is a case far from optimal as flotation tanks at industrial scale are generally connected in series, and therefore, the performance of tanks down the bank is directly affected by the performance of those upstream. It should be also noted that the optimisation strategy was tested in a closed loop, in which the only manipulated variable was the air flowrate, maintaining reagent conditions constant and pulp flowrates equal to zero, which is clearly not comparable with flotation at industrial scale.

As flotation froths play an important role in the flotation performance, much research has focused on modelling the phenomena occurring in this phase, specially focused on simulation purposes (i.e. analysis and design).For example, foam physics models developed by Verbist et al. (1996); Leonard and Lemlich (1965) have been further extended to describe flotation froths (Neethling et al., 2000; Neethling and Cilliers, 2002; Neethling et al., 2002, 2003; Neethling and Cilliers, 2009). These models aim to describe both internal behaviour and overall performance.

It must be noted that some of these models are not directly applicable to flotation control as they take the form of PDEs and are too complex to solve for control purposes. However, they have also been simplified to an extent that could make them amenable to control, even though they were developed assuming steady state. For example, in Oosthuizen and Craig (2019), the potential use of non-linear flotation models for control has been investigated and demonstrated. The benefit of such an approach lies in that the concept of PAR implies that there is an optimal operating point as recovery goes through a maximum when air rate is varied (i.e. a non-linear model is required). A brief introduction to some simplified froth models that could be used in future MPC studies for flotation control is presented below.

Water recovery: The simplified models developed in Neethling et al. (2003) are focused on predicting the amount of liquid collected in the concentrate (i.e. water recovery), which is directly related to the amount of gangue collected and, therefore, to the grade of valuable ore in the concentrate. To do so, a model that relates the amount of water collected with the air flowrate, air recovery and bubble size was developed:

$$\begin{aligned} &\text{if } \alpha < \tfrac{1}{2} : Q_l = \tfrac{A J_{\mathrm{g}}^2 \lambda}{k_1}(1-\alpha)\alpha \\ &\text{if } \alpha \geqslant \tfrac{1}{2} : Q_l = \tfrac{A J_{\mathrm{g}}^2 \lambda}{4k_1}, \end{aligned} \tag{58}$$

where α is the air recovery (in most rougher and scavenger cells α is less than 0.5), Q_l is the upwards liquid flowrate in the froth, A is the flotation cell cross-sectional area, J_g is the superficial gas velocity, and λ is the length of the Plateau borders per volume of froth, which is related with bubble size as shown in Eq.(59):

$$\lambda \propto \frac{1}{d_{\mathrm{BF}}^2}, \tag{59}$$

where d_{BF} is the bubble size in the froth phase. The constant $k_1$is a result of the force balance between gravity and viscosity, and it is defined as Eq.(60):

$$k_1 = \frac{\rho_p g}{3C_{\mathrm{PB}}\mu}, \tag{60}$$

where ρ is the pulp density, g is gravity, C_{pb} is the drag coefficient, which is a function of interfacial mobility, taking a value of 49 for immobile interfaces, which will be an appropriate value for many particle laden flotation froths, and μ is the pulp viscosity.

Entrainment factor: The performance of the froth flotation process is partly determined by the concentrate grade achieved. This is directly related to the entrainment of gangue material in the concentrate. It has been demonstrated that the amount of gangue entrained is proportional to the water recovery presented in Eq.(58). This proportionality is known as the entrainment factor. Neethling and Cilliers (2009) developed a simplified model for the entrainment factor as a function of operating conditions, such as froth depth and air rate:

$$\begin{array}{l} \text{if } \alpha < \frac{1}{2} : Ent \approx \exp\left(-\frac{v_{\mathrm{set}}^{1.5}\, h_{\mathrm{f}}}{D_{\mathrm{Axial}}\sqrt{J_g \alpha(1-\alpha)}}\right) \\ \text{if } \alpha \geq \frac{1}{2} : Ent \approx \exp\left(-\frac{2v_{\mathrm{set}}^{1.5}\, h_{\mathrm{f}}}{D_{\mathrm{Axial}}\sqrt{J_g}}\right) \end{array}, \tag{61}$$

where α is the air recovery, v_{set} is the settling velocity, h_f is the froth depth, D_{axial} is the axial dispersion, and J_g is the superficial gas velocity, i.e. Q_{air}/A_{cell}. The settling velocity, v_{set}, is assumed constant since the solid concentration is generally low. This velocity can be calculated as in Eq.(62). The axial dispersion, D_{axial}, is calculated as in Eq.(63).

$$v_{\mathrm{set}} \approx \frac{1}{3}\frac{g\,(\rho_{\mathrm{S}} - \rho_l)\, d_{\mathrm{p}}^2}{18\mu}, \tag{62}$$

$$D_{\mathrm{Axial}} \approx \frac{J_{\mathrm{g}}^{1.5}}{\sqrt{k_1(\sqrt{3} - \pi/2) Pe}}, \tag{63}$$

where Pe is the Péclet number, which can be assumed 0.15 (Neethling and Cilliers, 2009).

The entrainment factor is important to predict the entrained solids recovery from the estimated water recovery (from Eq.(58)). In Neethling and Cilliers (2009), it was demonstrated that while particle size has a strong influence on the entrainment factor, there is no direct dependence of it on the overflowing bubble sizes.

Froth recovery: Froth recovery is defined as the fraction of the material that enters the froth attached to the bubbles that reports to the concentrate, rather than dropping back into the pulp (Finch and Dobby, 1991; Neethling and Cilliers, 2008). By including the froth recovery into control strategies, the performance of predictive control strategies could be enhanced as it is related to the particle detachment, as well as the behaviour of unattached particles. Froth recovery could be included into control strategies by using a simplified model developed by Neethling and Cilliers (2008). This simple froth recovery model is a function of operating variables, such as superficial gas velocity, J_g, air recovery, α, and bubble sizes, as follows:

$$\begin{aligned} \text{if } \alpha < \tfrac{1}{2} : R_{\text{Froth}} &\approx \left(\tfrac{\alpha(1-\alpha)J_g}{v_{\text{set}}}\right)^{\frac{f}{2}} \left(\tfrac{d_{\text{b, int}}}{d_{\text{BF, out}}}\right)^{f} \\ \text{if } \alpha \geq \tfrac{1}{2} : R_{\text{Froth}} &\approx \left(\tfrac{J_g}{4v_{\text{set}}}\right)^{\frac{f}{2}} \left(\tfrac{d_{\text{b, int}}}{d_{\text{BF, out}}}\right)^{f} \end{aligned} , \tag{64}$$

where f is the fraction of material that becomes detached from the bubble interface during a coalescence event, $d_{b,\text{int}}$ is the bubble size in the pulp-froth interface, and $d_{BF,\text{out}}$ is the bubble size in the froth phase, overflowing the cell lip.

Although there have been attempts to develop simple froth models, such as those presented above, there is still a gap in our knowledge on how to include this type of simplified models into predictive control strategies. It should be possible to include these simplified models as a complement to an existing dynamic flotation model. Future work is therefore needed, and it should focus on the implementation of this approach, which could eventually lead to better performance of flotation MPC strategies.

Another approach that has attracted much attention has been the development of models based on hydraulic balances, considering variables that are commonly measured in industrial flotation cells, such as the inlet and outlet pulp flowrates. Hydraulic-based models for flotation control is the focus of the next section.

3.2.2. Hydraulic models

Hydraulic models are based on the continuity equation. Jämsä-Jounela et al. (2003) used this principle in order to implement a pulp level control strategy for six flotation cells. One SISO (single-input single-output) controller and three different MIMO (multi-input multi-output) controllers were tested. In order to determine which type of controller is more suitable for pulp levels, simulations in Matlab (Simulink) were performed, finding that SISO controllers are considerably less efficient in their ability to control the cell levels than MIMO controllers. Dynamic phenomenological models to predict the pulp levels in the cells, as shown in Eq.(65) for the first cell, Eq.(66) for the 2nd to $(n-1)$ cells and Eq.(67) for the last one, were proposed. These equations are valid when there is a tailings valve for each tank, as shown in Fig. 7, and when the cross-sectional area of the cell is constant.

$$\frac{dh_{p_1}}{dt} = \frac{q - K_v C_\text{v}(u_1)\sqrt{h_{p_1} - h_{p_2} + \Delta h_{p_1}}}{A_1}, \tag{65}$$

$$\begin{aligned}\frac{dh_{p_j}}{dt} =& \frac{K_{V_{j-1}} C_v(u_{j-1})\sqrt{h_{p_{j-1}} - h_j + \Delta h_{p_{j-1}}}}{A_j} \\ & - \frac{K_V C_\text{v}(u_j)\sqrt{h_{p_j} - h_{p_{j+1}} + \Delta h_{p_j}}}{A_j},\end{aligned} \tag{66}$$

$$\begin{aligned}\frac{dh_{p_n}}{dt} =& \frac{K_{V_{j-1}} C_\text{v}(u_{j-1})\sqrt{h_{p_{j-1}} - h_n + \Delta h_{p_{j-1}}}}{A_n} \\ & - \frac{K_V C_\text{v}(u_n)\sqrt{h_{p_n} + \Delta h_{p_n}}}{A_n},\end{aligned} \tag{67}$$

where h_{p_1}, h_{p_j}, and h_{p_n} are the pulp level in the flotation cell number 1, 2 to $(n-1)$ and n, respectively. K_V is a proportional constant, C_v is the valve coefficient, and u_1, u_j and u_n are the control valve positions for the tailings flowrate from the cells 1, 2 to $(n-1)$ and n, respectively. Δh_p is the physical difference between two consecutive cells.

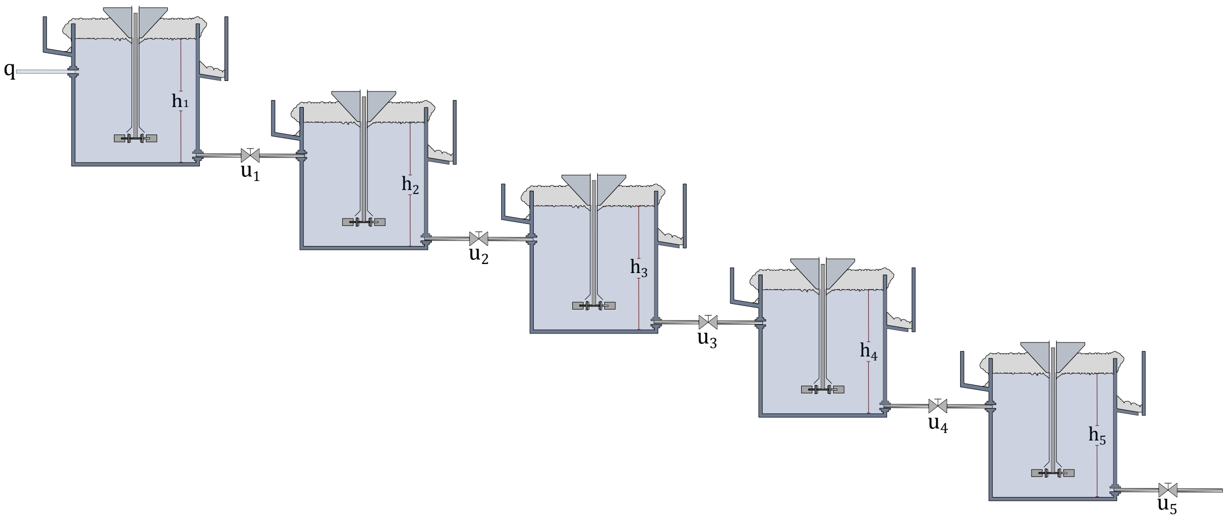

Figure 7: Schematic diagram of flotation cells. Adapted from Jämsä-Jounela et al. (2003)

Basic PI-controllers for level in every cell were used to evaluate the control strategies proposed, and only the feed flowrate was measured (flowrate into the first cell). In order to develop these models, the effect of air flowrate on the pulp level was explicitly ignored by Jämsä-Jounela et al. (2003). It was also assumed that froth height is negligible in comparison to the pulp level. However, it has been demonstrated that air flowrate directly affects the pulp level in aerated tanks such as those used in froth flotation (Shean et al., 2018) and, therefore, the effect of changes in air flowrate should not be ignored in future studies on flotation control, especially given the recent focus on optimising performance by varying the air flowrate into the cell.

Similar, but simpler hydraulic balances were proposed by Zaragoza and Herbst (1989), as shown in Eqs.(68) and (69) for the pulp and froth phase, respectively:

$$\frac{dV_{LP}}{dt} = Q_{FD} - Q_T - Q_E + Q_R, \tag{68}$$

$$\frac{dV_{LF}}{dt} = Q_E - Q_R - Q_C, \tag{69}$$

where Q_E is the flowrate of entrained water, Q_R is the flowrate of water draining back to the pulp, Q_C is the water leaving the flotation tank with the concentrate, Q_T is the tailings flowrate, Q_{FD} is the water fed to the cell, V_{LP} is the volume of the liquid in the pulp and V_{LF} is the volume of liquid in the froth. Kalman filters were used to implement the on-line estimation equations of the simplified models (i.e. Eqs.(47), (48), (68), and (69)) proposed by Zaragoza and Herbst (1989).

A hydraulic approach was also taken by Putz and Cipriano (2015) to calculate the dynamics of the pulp level (h_{p_j}) for each cell, j. The pulp level was determined from the hydraulic model developed by Jämsä-Jounela et al. (2003), but with the addition of logic variables δ_1^j (i.e. variables that can take a value of 0 or 1, depending on the conditions previously defined) as:

$$\frac{dh_{p_j}}{dt} = \frac{1}{A_j} \left(Q_{F_j} - Q_{T_j} - Q_{C_j} \right) \delta_1^j. \tag{70}$$

where A_j is the cross-sectional area of the cell j, and Q_{F_j}, Q_{T_j} and Q_{C_j} are the feed, tailings and concentrate flowrates from the cell j, respectively.

Unlike the model proposed by Jämsä-Jounela et al. (2003), the hydraulic model presented in Eq.(70) does not include the valve coefficient, and rather integrates logical rules as part of the hybrid models. In all previous hydraulic models presented, it was assumed that the change in the pulp level was the result of only the pulp flowrate into and out of the cell. However, it has been demonstrated that changes in the gas flowrate can also have an appreciable impact on the pulp height (Shean et al., 2018). These effects are linked to changes in (1) gas hold-up (Vinnett et al., 2014), and (2) bubble size (Gorain et al., 1995; Nesset et al., 2006).

The effect of air flowrate on pulp level control was studied by Shean et al. (2018), where a dynamic model was developed and validated in both a water-only system and a system with reagents. To carry out the model development, assumptions such as well-mixed tank, ideal gas law for the gas phase, and hydrostatic pressure within the tank, were taken. The change in pulp level was determined using Eq.(71). A relation between average gas hold-up (ε_{ave}) and the top of the tank gas hold-up (ε_g) was derived, as shown in Eq.(72).

$$\frac{dV_{gas}}{dt} = \frac{d\left(V_{\text{system}}\varepsilon_{Ave}\right)}{dt} = A\frac{d\left(h\varepsilon_{Ave}\right)}{dt}, \tag{71}$$

where:

$$\frac{\varepsilon_{Ave}}{\varepsilon_g} = X_\varepsilon \approx \frac{P_0}{\rho_{\text{p}} g\left(1-\varepsilon_g\right)h_p} \ln\left(\frac{\rho_{\text{p}} g\left(1-\varepsilon_g\right)h_p}{P_0} + 1\right). \tag{72}$$

Thus:

$$\frac{dV_{gas}}{dt} = A\frac{d\left(h_p\varepsilon_g X_\varepsilon\right)}{dt}. \tag{73}$$

The change in gas hold-up (ε_g) for each bubble size class i, can be determined by Eq.(74), which is a function of air flowrate (Q_A), feed flowrate (Q_F), and the total pulp out of the cell ($Q_{pulp,out}$), which is the sum of tailings and concentrate flowrates:

$$\begin{aligned}\frac{d}{dt}\left(\frac{X_\rho \varepsilon_{g_i} X_\varepsilon}{1-\varepsilon_{g,\text{total}} X_\varepsilon}\right) =& \frac{1}{h_0}\left[\frac{Q_\text{A}}{A} - v_\text{gas}\varepsilon_{g,i}\right] \\ &- \frac{1}{h_0}\left[\frac{Q_F}{A} - \frac{Q_\text{pulp,out}}{A}\right]\left(\frac{\varepsilon_{g_i} X_\varepsilon}{1-\varepsilon_{g,\text{total}} X_\varepsilon}\right)\end{aligned} \tag{74}$$

where v_{gas} is the upward gas velocity of the bubble from the pulp phase to the interface, which is a function of gas hold-up and the bubble size in the pulp phase (Eq.(75)):

$$v_{gas} = \frac{g d_{BP}^2 \rho_p}{18\mu}\left[1-\varepsilon_g\right]^{1.39}. \tag{75}$$

The term X_ρ is the ratio of the average to surface gas density, which can be calculated as follows:

$$\frac{\rho_{gAve}}{\rho_{g0}} = X_\rho \approx \frac{\frac{\rho_\text{p} g(1-\varepsilon_g)h_p}{P_0 \ln\left(\frac{\rho_\text{p} g(1-\varepsilon_g)h_p}{P_0}+1\right)} - \varepsilon_g}{1-\varepsilon_g}. \tag{76}$$

For a more in-depth description of the derivation of Eqs.(72) and (76), the reader is referred to the Appendix A in Shean et al. (2018). It should be noted that Eqs.(73) and (74) are in fact revised versions of those in Shean et al. (2018) since from Eq.(72) it can be seen that $\varepsilon_{Ave} = \varepsilon_0 X_\varepsilon$, rather than $\varepsilon_{Ave} = \frac{\varepsilon_0}{X_\varepsilon}$ as presented in the original paper. Although it has been demonstrated that the dynamic model in Eq.(74) presents an improvement in predicting pulp level changes, it has never been tested as part of a level control strategy. In fact, Eq.(74) could be implemented for a better control of the pulp level as it considers not only the effect of the pulp flowrate but also the effect of the air flowrate, specially when this variable is considered as one that is continuously manipulated. Nonetheless, it should be noted that only the effect of air flowrate on pulp level was validated at laboratory scale by Shean et al. (2018), and therefore there is still scope to validate the effect of pulp flowrate (Q_F and $Q_\text{pulp out}$).

Whereas hydraulic models, such as those proposed by Jämsä-Jounela et al. (2003); Zaragoza and Herbst (1989) and Putz and Cipriano (2015), consider the effect of operational variables (i.e. flowrates) that are typically directly measured, other phenomena within the pulp and/or froth phase that are difficult to measure are ignored, such as attachment/detachment processes, bubble coalescence, and liquid and solid, among others. The attachment/detachment phenomena, however, have been included when population balance models are taken into account for control strategies. In the next section, the population balance approach is discussed in detail.

3.2.3. Population balance models

Another approach to phenomenological modelling is the use of population balance models, which can be applied for both simulation and control purposes (Herbst and Harris, 2007). Mika and Fuerstenau (1969) described population balances for four states for particles in a flotation cell, as shown in Fig. 8, which are: (1) free in the pulp phase, (2) attached to bubbles in the pulp phase, (3) free in the froth phase (i.e. entrained), or (4) attached in the froth phase.

Eq.(77) is the general population balance equation that represents each of the four possible states (Herbst and Harris, 2007; Herbst and Flintoff, 2012; Jovanović et al., 2015), for every mineral particle size i, and mineral particle composition j.

$$\frac{\partial V\psi_j}{\partial t} = \psi_{\mathrm{j,IN}}Q_{\mathrm{F}} - \psi_{\mathrm{j,OUT}}Q_{\mathrm{pulp\ out}} - \sum_{i=1}^{k} k_{ji}\psi_j V, \tag{77}$$

where ψ_j is the concentration of mineral particles, V is the volume of the flotation cell, Q_F and $Q_{\mathrm{pulp\ out}}$ are the volumetric flowrate into and out of the cell, respectively, and k_{ji} is the particle transfer rate between the states. Each of the four states established in the population balance was modelled as shown in Eqs.(78) to (81), as follows:

1. Free particles in the pulp phase: Eq.(78) shows the population balance for unattached particles in the pulp phase, at time t. This balance indicates that the accumulation of free particles of size i and mineralogical species j in the pulp phase ($\frac{d}{dta}(V_{LP}\psi_{ij}^{LP})$) is a function of the rate of attachment ($K_{ij}^{PAT}V_{LP}\psi_{ij}^{LP}$) and detachment ($K_{ij}^{PDT}V_{BP}\psi_{ij}^{BP}$) for particles in the pulp, the feed of particles into the flotation cell ($Q_{Feed}\psi_{ij}^{Feed}$), the flowrate of particles leaving the cell with the tailings ($Q_T\psi_{ij}^{LP}$), the flowrate of particles

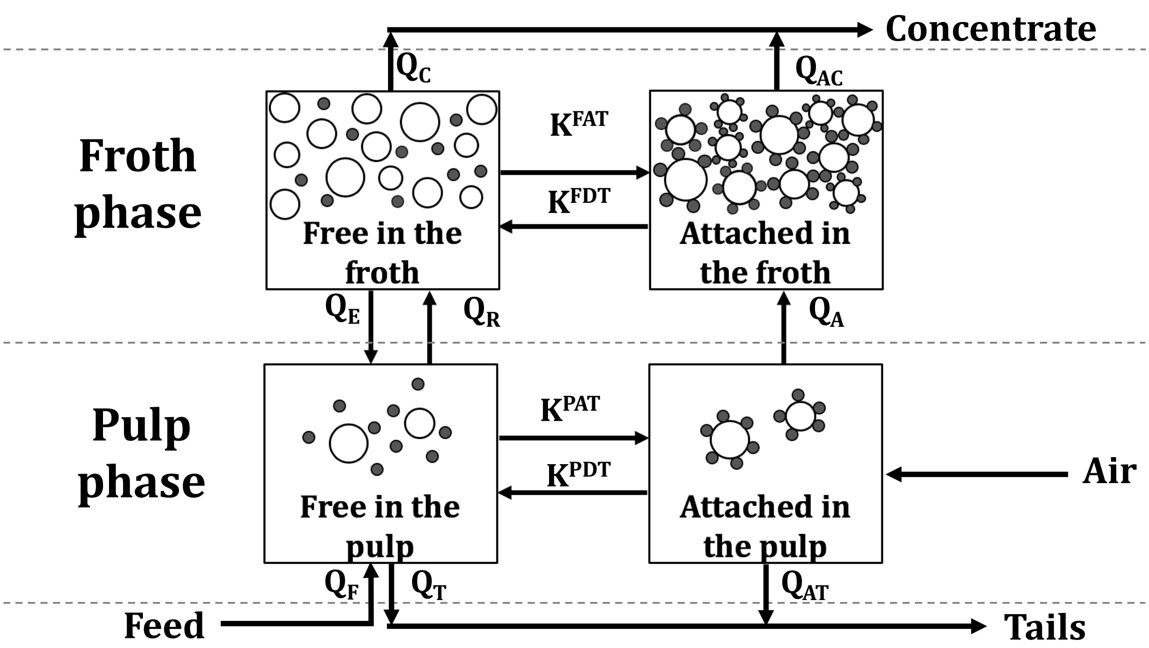

Figure 8: Four states for particles in a flotation cell: (1) Free particles in the pulp phase, (2) Attached particles in the pulp phase, (3) Free particles in the froth phase and (4) attached particles in the froth phase. (Adapted from Herbst and Harris (2007); Jovanović et al. (2015)).

draining from the froth carried by water ($K_{ij}^{R}Q_R\psi_{ij}^{LF}$), and the flowrate of entrained particles into the froth ($Q_E\psi_{ij}^{LP}$).

$$\begin{aligned}\frac{d}{dt}\left(V_{LP}\psi_{ij}^{LP}\right) &= -K_{ij}^{PAT}V_{LP}\psi_{ij}^{LP} + K_{ij}^{PDT}V_{BP}\psi_{ij}^{BP} \\ &+Q_{Feed}\psi_{ij}^{Feed} - Q_T\psi_{ij}^{LP} + K_{ij}^{R}Q_R\psi_{ij}^{LF} - Q_E\psi_{ij}^{LP}\end{aligned} \tag{78}$$

2. Attached particles in the pulp phase: Eq.(79) shows the population balance for particles that are attached to a bubble in the pulp phase, at time t. This balance indicates that the accumulation of particles attached to bubbles in the pulp phase ($\frac{d}{dt}(V_{LP}\psi_{ij}^{BP})$) is a function of the rate of attachment ($K_{ij}^{PAT}V_{LP}\psi_{ij}^{LP}$) and detachment ($K_{ij}^{PDT}V_{BP}$) of particles, the transport of particles attached to bubbles to the froth ($Q_A\psi_{ij}^{BP}$), and the

particles attached to bubbles leaving the cell through tailings ($Q_{AT}\psi_{AT}^{BP}$).

$$\frac{d}{dt}\left(V_{LP}\psi_{ij}^{BP}\right) = K_{ij}^{PAT}V_{LP}\psi_{ij}^{LP} - K_{ij}^{PDT}V_{BP} \\ \psi_{ij}^{BP} + Q_A\psi_{ij}^{BP} - Q_{AT}\psi_{ij}^{LP} \tag{79}$$

3. Free particles in the froth phase: Eq.(80) shows the population balance for particles entrained with the liquid in the froth phase. This balance indicates that the accumulation of free particles in the froth phase ($\frac{d}{dt}(V_{LF}\psi_{ij}^{LF})$) is a function of the rate of attachment ($K_{ij}^{FAT}V_{LF}\psi_{ij}^{LF}$) and detachment ($K_{ij}^{FDT}V_{BF}\psi_{ij}^{BF}$) of particles in the froth phase, the rate of particles carried due to water entrainment from the pulp ($Q_E\psi_{ij}^{LP}$), the rate of particles carried out of the froth due to water drainage ($K_{ij}^{R}Q_R\psi_{ij}^{LF}$), and the rate of non-attached particles in the froth that overflows into the concentrate launder ($Q_C\psi_{ij}^{LF}$).

$$\frac{d}{dt}\left(V_{LF}\psi_{ij}^{LF}\right) = K_{ij}^{FAT}V_{LF}\psi_{ij}^{LF} + K_{ij}^{FDT}V_{BF}\psi_{ij}^{BF} \\ +Q_E\psi_{ij}^{LP} - K_{ij}^{R}Q_R\psi_{ij}^{LF} - Q_C\psi_{ij}^{LF} \tag{80}$$

4. Attached particles in the froth phase: Eq.(81) shows the population balance for those particles in the froth that are attached to bubbles. This balance indicates that the accumulation of attached particles in the froth phase ($\frac{d}{dt}(V_{BF}\psi_{ij}^{BF})$) is a function of the rate of attachment ($K_{ij}^{FAT}V_{LF}\psi_{ij}^{LF}$) and detachment ($K_{ij}^{FDT}V_{BF}\psi_{ij}^{BF}$) of particles in the froth phase, the rate of particles that are carried by air bubbles from the pulp phase ($Q_A\psi_{ij}^{BP}$), and the rate of particles that are attached into bubbles in the froth that reports to the concentrate ($Q_{AC}\psi_{ij}^{BF}$).

$$\frac{d}{dt}\left(V_{BF}\psi_{ij}^{BF}\right) + k_{ij}^{FDT}V_{BF}\psi_{ij}^{BF} - k_{ij}^{FAT}V_{LF}\psi_{ij}^{LF} \\ = Q_A\psi_{ij}^{BP} - Q_{AC}\psi_{ij}^{BF} \tag{81}$$

Parameters, such as rate constants, water entrainment/drainage and water into the concentrate, can be determined empirically as shown in Section 3.1, in Eqs.(23) to (33). In the study carried out by Bascur (1982), phenomenological models were developed with a focus on automatic control, by considering three types of particles: free valuable minerals, free gangue, and locked particles.

The aforementioned population balance models are used to represent the attachment and detachment phenomena, as well as the solids transfer between the pulp phase and froth phase. However, these models do not fully represent the phenomena that occur in a flotation cell, specially in the froth phase. To date, physics-based models for the froth phase have not been developed for control purposes. While phenomenological models based on kinetics and population balances work well to represent the pulp phase, they do not adequately represent the froth phase, with the assumption of a well-mixed system being particularly problematic. They also do not incorporate the important stability effects, such as bubble coalescence and bursting which are important drivers in the overall performance of froths.

3.3. Hybrid models

Hybrid models are used to represent a process by using both continuous and discrete variables. The discrete variables are logic rules that represent different operating conditions of the process (also known as "modes") that generate changes in the continuous variables. The first hybrid model predictive control for flotation, based on PWARX (PieceWise AutoRegresive eXogenous) models (Heemels et al., 2001), was developed by Putz and Cipriano (2015). The PWARX system was used to approximate non-linear process dynamics, such as the froth flotation process, by using linearised models at different operating conditions (Sontag, 1981).

In order to implement the hybrid MPC, Putz and Cipriano (2015) defined three modes, as shown in Fig. 9, as follows: (1) flotation cell with the presence of pulp and froth phases, but no concentrate overflow, (2) normal operation (presence of the pulp and froth phases, as well as concentrate overflow), and (3) operation with overflow of the pulp phase (i.e. no presence of the froth phase). In order to simplify the formulation, only the first two operating conditions were taken into account, with the third one considered as an operating ($h_p^i \leqslant h_{max}^i$, i.e. pulp height cannot be greater than the cell height).

In order to implement the hybrid MPC, assumptions were made such as perfect mixing, constant air flowrate, and constant tank cross-sectional area, and considering two mineralogical classes (high and low chalcopyrite grade). This last consideration on mineralogical

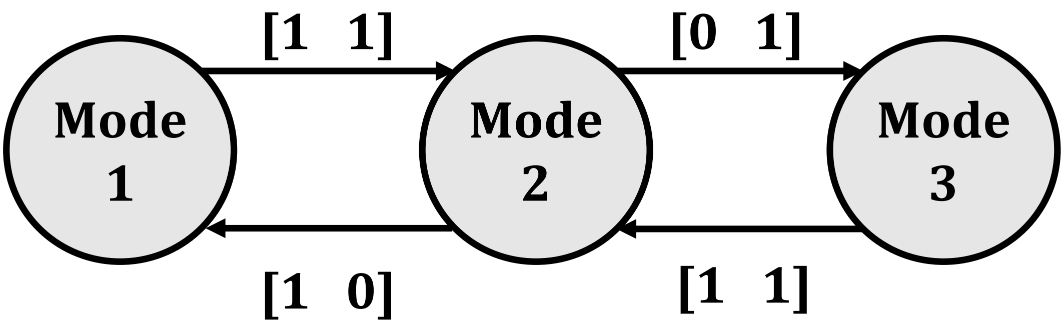

Figure 9: Operating conditions in a flotation tank proposed by Putz and Cipriano (2015). Mode 1 represents an operation with the presence of both pulp and froth phases, without froth overflow; Mode 2 represents a normal operation with the presence of both pulp and froth phases, and also froth overflow; and Mode 3 represents an operation with the presence of pulp phase only, with overflow of pulp phase at the top of the flotation cell.

classes is, in fact, not ideal as the mineralogy have a significant impact on the concentrate economic value. More realistic results could have been obtained if a distributed mineralogy, for example, was taken into account instead.

Two logical variables were defined as δ_1^j and δ_2^j. Depending on the operating conditions, the logical variables can take the value of 0 or 1. Eq.(82) and Eq.(83) show the logical rules that were defined to implement the hybrid MPC by Putz and Cipriano (2015).

$$\delta_1^j = \begin{cases} 1 & \text{if } h_p^j \leqslant h_{\max}^j \\ 0 & \text{if } h_p^j > h_{\max}^j \end{cases}, \tag{82}$$

$$\delta_2^j = \begin{cases} 1 & \text{if } h_p^j + h_f^i > h_{\max}^j \\ 0 & \text{if } h_p^j + h_f^j \leqslant h_{\max}^j \end{cases} \tag{83}$$

where h_p^j and h_f^j are the pulp height and froth depth of the cell j, respectively. Both logical variables δ_1^j and δ_2^j, can be grouped in a vector that contains each value, as $\begin{bmatrix} \delta_1^j & \delta_2^j \end{bmatrix}$. The three operating conditions previously defined and their respective logical states are presented in Fig. 9. The use of only logical rules, however, was not enough to effectively implement a model predictive controller. For this reason, empirical (Eqs.(6), (7), (15), and (16)) and phenomenological models (kinetic balances: Eqs.(45) and (46); hydraulic model: Eq.(70)) were also implemented by Putz and Cipriano (2015).

Simulations were run to test the proposed hybrid flotation models, with the feed flowrate and the feed grade as the measured disturbance variables. The controlled variable was the pulp height and the final tailings grade, which was manipulated by controlling the position of the tailings valve. The effect that air flowrate and regent addition rate were thus ignored in terms of their influence on the pulp level. The control aim was to minimise the error between a reference and the final tail grade, while minimising the variations in the manipulated variables.

Although other hybrid models have been developed for analysis or design purposes, such as Gupta et al. (1999), to the knowledge of the authors, the hybrid model implemented into a control strategy by Putz and Cipriano (2015) is the only one of its kind and, thus, no comparison can be made with other control studies. It should, however, be noted that is important to identify gaps in knowledge that can lead to further research and, hence, to find a way to optimally control the flotation process.

4. Conclusions

Numerous studies have established that the efficiency of flotation control can be improved by using advanced controllers, such as Model Predictive Control (MPC). MPC is a powerful control strategy for complex processes such as froth flotation. This control strategy optimises the process by using explicit models able to predict its outputs, minimising a cost function that depends on process variables and process constraints. The most crucial part of this control strategy is the model development itself, specially in a complex process such as froth flotation, due to its dynamic nature and the fact it can be affected by a great number of variables.

This review has, for the first time in the literature, classified and analysed models used for flotation MPC strategies, providing a framework for future studies. The models used for

MPC strategies were classified as empirical, phenomenological or hybrid models. Empirical models have been mainly developed to determine flotation rate constants, drainage rate constant, concentrate volumetric flowrate, among other parameters, by using fits to plant data. Although these models are cost-effective, they can only be used when the process is under a well-known range of operating conditions and, therefore, their robustness outside that range is highly debatable. Phenomenological models, as well as hybrid models, can be applied to into any flotation system since they are derived from first principles. In this review, phenomenological models were classified into three types: kinetic, hydraulic and population balance models.

The analysis of the literature on the topic has shown that little evidence on successful MPC implementation in flotation at industrial scale is available. There remains a need for further research to enhance modelling for flotation control purposes. To date, MPC studies have tended to use kinetic models to phenomenologically represent the attachment-detachment of mineral particles in the pulp phase and the froth phase. While kinetic models can accurately represent the phenomena in the pulp phase, these models are not suitable for the froth phase, as more complex phenomena are involved. In fact, froth phase phenomena such as bubble coalescence, bubble bursting, and liquid and solid motion, are key drivers of froth performance. There is therefore an important opportunity to develop suitable models that take into account the physics of the froth phase and can be implemented into MPC strategies. Addressing the gap between models for the pulp phase and for the froth phase suitable to be implemented into MPC strategies will pave the way for improving the overall performance of the flotation process.

Acknowledgements

Paulina Quintanilla would like to acknowledge the National Agency for Research and Development (ANID) for funding this research with a scholarship from “Becas Chile”.

References

Al-Thyabat, S., 2008. On the optimization of froth flotation by the use of an artificial neural network. Journal of China University of Mining and Technology 18, 418–426. doi:10.1016/S1006-1266(08)60087-5.

Aldrich, C., Marais, C., Shean, B., Cilliers, J., 2010. Online monitoring and control of froth flotation systems with machine vision: A review. International Journal of Mineral Processing 96, 1–13. doi:10.1016/J.MINPRO.2010.04.005.

Alves dos Santos, N., Savassi, O., Peres, A.E.C., Martins, A.H., 2014. Modelling flotation with a flexible approach âĂŞ Integrating different models to the compartment model. Minerals Engineering 66-68, 68–76. URL: https://www.sciencedirect.com/science/article/pii/S0892687514001769, doi:10.1016/J.MINENG.2014.05.007.

Arbiter, N., Harris, C.C., 1962. Flotation Kinetics, in: Froth Flotation. d. w. fuer ed.. Edwards Brothers Inc, New York, pp. 215–246.

Bartolacci, G., Ourriban, M., Bouajila, A., Gomez, C., Finch, J., Goyette, G., 2008. On-line use of hydrodynamic sensors to improve metallurgical performance of flotation machine., in: Gomez, C., Kuyvenhoven, R., Casali, A. (Eds.), V International Mineral Processing Seminar, PROCEMIN, Santiago, Chile. pp. 357–366.

Bartolacci, G., Pelletier, P., Tessier, J., Duchesne, C., Bossé, P.A., Fournier, J., 2006. Application of numerical image analysis to process diagnosis and physical parameter measurement in mineral processesâĂŤPart I: Flotation control based on froth textural characteristics. Minerals Engineering 19, 734–747. doi:10.1016/J.MINENG.2005.09.041.

Bascur, O.A., 1982. Modelling and computer control of a flotation cell. University of Utah, Salt Lake City .

Bergh, L., Yianatos, J., 1994. Experimental studies on flotation column dynamics. Minerals Engineering 7, 345–355. doi:10.1016/0892-6875(94)90075-2.

Bergh, L., Yianatos, J., 1996. Hierarchical control strategy in columns at El Teniente, in: Proceedings of the International Symposium on Column Flotation, Montreal, Canada. pp. 369–380.

Bergh, L., Yianatos, J., Pino, C., 2013. Advances in developing supervisory control strategies for flotation plants. IFAC Proceedings Volumes 46, 110–115. doi:10.3182/20130825-4-US-2038.00003.

Bergh, L.G., 2016. Artificial Intelligence in Mineral Processing Plants : An Overview. International Conference on Artificial Intelligence: Technologies and Applications (ICAITA 2016) , 278–281.

Bergh, L.G., Yianatos, J.B., 2003. Flotation column automation: State of the art. Control Engineering Practice doi:10.1016/S0967-0661(02)00093-X.

Bergh, L.G., Yianatos, J.B., 2011. The long way toward multivariate predictive control of flotation processes. Journal of Process Control 21, 226–234. doi:10.1016/j.jprocont.2010.11.001.

Bergh, L.G., Yianatos, J.B., Acuña, C.A., Pérez, H., López, F., 1999. Supervisory control at Salvador flotation columns. Minerals Engineering 12, 733–744. doi:10.1016/S0892-6875(99)00060-6.

Bergh, L.G., Yianatos, J.B., Leiva, C.A., 1998. Fuzzy supervisory control of flotation columns. Minerals Engineering doi:10.1016/s0892-6875(98)00059-4.

Bertsekas, D.P., 1995. Dynamic Programming and Optimal Control. Athena Scientific.

Bonifazi, G., Serranti, S., Volpe, F., Zuco, R., 2001. Characterisation of flotation froth colour and structure by machine vision. Computers & Geosciences 27, 1111–1117. doi:10.1016/S0098-3004(00)00152-7.

Bordons, C., 2000. Control predictivo: metodología, tecnología y nuevas perspectivas. Technical Report. Universidad de Sevilla. Aguadulce, Almería.

Bouchard, J., Desbiens, A., del Villar, R., Nunez, E., 2009. Column flotation simulation and control: An overview. Minerals Engineering 22, 519–529. URL: http://dx.doi.org/10.1016/j.mineng.2009.02.004, doi:10.1016/j.mineng.2009.02.004.

Camacho, E.F., Bordons, C., 2007. Model Predictive Control. doi:10.1007/978-0-85729-398-5, arXiv:arXiv:1011.1669v3.

Carr, D., Dixon, A., Tiili, O., 2009. Optimising Large Flotation Cell Performance Through Advanced Instrumentation and Control, in: Tenth Mill Operator's Conference, Adelaide, SA. pp. 299–304.

Casali, A., Gonzalez, G., Agusto, H., Vallebuona, G., 2002. Dynamic simulator of a rougher flotation circuit for a copper sulphide ore. Minerals Engineering 15, 253–262. doi:10.1016/S0892-6875(02)00016-X.

Chelgani, S.C., Shahbazi, B., Rezai, B., 2010. Estimation of froth flotation recovery and collision probability based on operational parameters using an artificial neural network. International Journal of Minerals, Metallurgy and Materials 17, 526–534. doi:10.1007/s12613-010-0353-1.

Cipriano, A., Guarini, M., Vidal, R., Soto, A., Sepúlveda, C., Mery, D., Briseño, H., 1998. A real time visual sensor for supervision of flotation cells. Minerals Engineering doi:10.1016/s0892-6875(98)00031-4.

Citir, C., Aktas, Z., Berber, R., 2003. Off-line image analysis for froth flotation of coal. Computer Aided Chemical Engineering 14, 605–610. doi:10.1016/S1570-7946(03)80182-7.

Cubillos, F.A., Lima, E.L., 1997. Identification and optimizing control of a rougher flotation circuit using an adaptable hybrid-neural model. Minerals Engineering 10, 707–721. doi:10.1016/s0892-6875(97)00050-2.

Del Villar, R., Grégoire, M., Pomerleau, A., 1999. Automatic control of a laboratory flotation column. Minerals Engineering 12, 291–308. doi:10.1016/s0892-6875(99)00007-2.

Desbiens, A., Hodouin, D., Mailloux, M., 1998. Nonlinear Predictive Control of a Rougher Flotation Unit Using Local Models. IFAC Proceedings Volumes 31, 287–292. URL: http://dx.doi.org/10.1016/S1474-6670(17)35893-7, doi:10.1016/S1474-6670(17)35893-7.

Desbiens, A., Hodouin, D., Najim, K.I., Flament, F., Universitaire, C., Gk, C., 1994. Long-range predictive control of a rougher flotation unit. Minerals Engineering 7, 21–37.

Desbiens, A., Hodouin, D., Plamondon, E., 2000. Global predictive control: A unified control structure for decoupling setpoint tracking, feedforward compensation and disturbance rejection dynamics. IEE Proceedings-Control Theory and Applications 147, 465–475. doi:10.1049/ip-cta:20000443.

Dinariev, O.Y., Evseev, N.V., 2018. Modelling of flotation processes by density functional hydrodynamics. Minerals Engineering doi:10.1016/j.mineng.2018.06.013.

Faulkner, B., 1966. Computer control improves metallurgy at Tennessee Copper's flotation plant. Mining Engineering 18, 53–57.

Ferreira, J.P., Loveday, B.K., 2000. Improved model for simulation of flotation circuits. Minerals Engineering doi:10.1016/S0892-6875(00)00129-1.

Finch, J.A., Dobby, G.S., 1991. Column flotation: A selected review. Part I. International Journal of Mineral Processing doi:10.1016/0301-7516(91)90062-N.

Forbes, G., 2007. Texture and bubble size measurements for modelling concentrate grade in flotation froth systems. Phd thesis. University of Cape Town.

Fu, Y., Aldrich, C., 2019. Flotation froth image recognition with convolutional neural networks. Minerals Engineering 132, 183–190. doi:10.1016/J.MINENG.2018.12.011.

Garcia-Zuniga, H., 1935. The efficiency obtained by flotation is an exponential funcion of time. Soc. Nac. Minera 47, 83–86.

Gharai, M., Venugopal, R., 2016. Modeling of flotation process - An overview of different approaches. Mineral Processing and Extractive Metallurgy Review 37, 120–133. doi:10.1080/08827508.2015.1115991.

Gomez, C.O., Cortés-López, F., Finch, J.A., 2003. Industrial testing of a gas holdup sensor for flotation systems. Minerals Engineering doi:10.1016/S0892-6875(03)00083-9.

Gorain, B.K., Franzidis, J.P., Manlapig, E.V., 1995. Studies on impeller type, impeller speed and air flow rate in an industrial scale flotation cell - Part 1: Effect on bubble size distribution. Minerals Engineering doi:10.1016/0892-6875(95)00025-L.

Gupta, S., Liu, P.H., Svoronos, S.A., Sharma, R., Abdel-Khalek, N.A., Cheng, Y., El-Shall, H., 1999. Hybrid first-principles/neural networks model for column flotation. AIChE Journal 45, 557–566. doi:10.1002/aic.690450312.

Gupta A., Yan D.S., 2006. Chapter 18. Process Control. Mineral Processing Design and Operation , 622—-671doi:10.1016/B978-044451636-7/50019-X.

Hadler, K., Cilliers, J.J., 2009. The relationship between the peak in air recovery and flotation bank performance. Minerals Engineering doi:10.1016/j.mineng.2008.12.004.

Hadler, K., Smith, C.D., Cilliers, J.J., 2010. Recovery vs. mass pull: The link to air recovery. Minerals Engineering 23, 994–1002. URL: http://dx.doi.org/10.1016/j.mineng.2010.04.007, doi:10.1016/j.mineng.2010.04.007.

Heemels, W.P.M.H., De Schutter, B., Bemporad, A., 2001. Equivalence of hybrid dynamical models. Automatica doi:10.1016/S0005-1098(01)00059-0.

Herbst, J.A., Flintoff, B., 2012. Recent Advances in Modeling, Simulation, and Control of Mineral Processing Operations, in: Separation Technologies for Minerals, Coal, and Earth Resources, pp. 667–680.

Herbst, J.A., Harris, M., 2007. Modeling and Simulation of Industrial Flotation Processes, in: Froth Flotation: A Century of Innovation, pp. 757–777.

Herbst, J.A., Pate, W.T., Oblad, A.E., 1992. Model-based control of mineral processing operations. Powder Technology 69, 21–32.

Hodouin, D., 2011. Methods for automatic control, observation, and optimization in mineral processing plants. Journal of Process Control 21, 211–225. doi:10.1016/j.jprocont.2010.10.016.

Hodouin, D., Jämsä-Jounela, S.L., Carvalho, M.T., Bergh, L., 2001. State of the art and challenges in mineral processing control. Control Engineering Practice 9, 995–1005. doi:10.1016/S0967-0661(01)00088-0.

Holtham, P., Nguyen, K., 2002. On-line analysis of froth surface in coal and mineral flotation using JKFrothCam. International Journal of Mineral Processing 64, 163–180. doi:10.1016/S0301-7516(01)00070-9.

Hsu, K.â., Gupta, H.V., Sorooshian, S., 1995. Artificial Neural Network Modeling of the RainfallâĂŘRunoff Process. Water Resources Research doi:10.1029/95WR01955.

Humaloja, J.P., Dubljevic, S., 2018. Linear Model Predictive Control for Schrödinger Equation. Proceedings of the American Control Conference 2018-June, 2569–2574. doi:10.23919/ACC.2018.8431686.

Hyötyniemi, H., Ylinen, R., 2000. Modeling of visual flotation froth data. Control Engineering Practice 8, 313–318. doi:10.1016/S0967-0661(99)00187-2.

Jahedsaravani, A., Marhaban, M.H., Massinaei, M., Saripan, M.I., Noor, S.B., 2016. Froth-based modeling and control of a batch flotation process. International Journal of Mineral Processing 146, 90–96. doi:10.1016/j.minpro.2015.12.002.

Jämsä-Jounela, S.L., Dietrich, M., Halmevaara, K., Tiili, O., 2003. Control of pulp levels in flotation cells. Control Engineering Practice 11, 73–81. doi:10.1016/S0967-0661(02)00142-9.

Jovanović, I., Miljanović, I., 2015. Contemporary advanced control techniques for flotation plants with mechanical flotation cells - A review. Minerals Engineering 70, 228–249. doi:10.1016/j.mineng.2014.09.022.

Jovanović, I., Miljanović, I., Jovanović, T., 2015. Soft computing-based modeling of flotation processes âĂŞ A review. Minerals Engineering 84, 34–63. doi:10.1016/J.MINENG.2015.09.020.

Kelsall, D., 1961. Application of probability in the assessment of flotation systems. Bull. Institution of Mining and Metallurgy 650, 191–204.

Kracht, W., Gomez, C.O., Finch, J.A., 2008. Controlling bubble size using a frit and sleeve sparger. Minerals Engineering 21, 660–663. doi:10.1016/j.mineng.2007.12.009.

Laurila, H., Karesvuori, J., Tiili, O., 2002. Strategies for Instrumentation and Control of Flotation Circuits, in: Mineral Processing Plant Design, Practice and Control Proceedings, pp. 2174–2195.

Leonard, R., Lemlich, R., 1965. Laminar longitudinal flow between close-packed cylinders. J. Chem. Eng. Sci 20, 790–791.

Lewis, H., 1997. The foundations of fuzzy control. Plenum Press, New York.

Liao, Y., Liu, J., Wang, Y., Cao, Y., 2011. Simulating a fuzzy level controller for flotation columns. Mining Science and Technology doi:10.1016/j.mstc.2011.05.038.

Liu, J., MacGregor, J., Duchesne, C., Bartolacci, G., 2005. Flotation froth monitoring using multiresolutional multivariate image analysis. Minerals Engineering 18, 65–76. doi:10.1016/J.MINENG.2004.05.010.

Liu, J.J., MacGregor, J.F., 2008. Froth-based modeling and control of flotation processes. Minerals Engineering 21, 642–651. doi:10.1016/j.mineng.2007.12.011.

Lynch, A., Johnson, N., Manlapig, E., Thorne, C., 1981. Mineral and Caol Flotation Circuits - Their Simulation and Control. Netherlands.

Maciejovski, J., 2002. Predictive control with constraints. Prentice Hall.

Maldonado, M., 2010. Advances in Estimation and Control for Flotation Columns. Ph.D. thesis. Université Laval.

Maldonado, M., Desbiens, A., Del Villar, R., 2009. Potential use of model predictive control for optimizing the column flotation process. International Journal of Mineral Processing 93, 26–33. doi:doi:10.1016/j.minpro.2009.05.004.

Maldonado, M., Desbiens, A., Del Villar, R., Girgin, E., Gomez, C., 2008. On-line estimation of bubble size distributions using Gaussian mixture models, in: Kuyvenhoven, C., Casali, A. (Eds.), V International Mineral Processing Seminar, PROCEMIN, Santiago, Chile. pp. 389–398.

Maldonado, M., Desbiens, A., Del Villar, R., Poulin, E., Riquelme, A., 2010. Nonlinear control of bubble size in a laboratory otation column. volume 43. Cape Town. doi:10.3182/20100802-3-ZA-2014.00004.

Maldonado, M., Desbiens, A., Del Villar, R., Quispe, R., 2007a. Towards the optimization of flotation columns using predictive control. IFAC Proceedings Volumes (IFAC-PapersOnline) 12, 75–80. doi:10.3182/20070821-3-CA-2919.00011.

Maldonado, M., Sbarbaro, D., Lizama, E., 2007b. Optimal control of a rougher flotation process based on dynamic programming. Minerals Engineering 20, 221–232. doi:10.1016/j.mineng.2006.08.015.

Massinaei, M., Doostmohammadi, R., 2010. Modeling of bubble surface area flux in an industrial rougher column using artificial neural network and statistical techniques. Minerals Engineering doi:10.1016/j.mineng.2009.10.005.

Mckay, J., Inchausti, R., 1996. Expert supervisory control of flotation columns, in: Proceedings of the International Symposium on Column Flotation, Montreal, Canada. pp. 353–367.

Mesa, D., Brito-Parada, P.R., 2019. Scale-up in froth flotation: A state-of-the-art review. Separation and Purification Technology 210, 950–962. doi:10.1016/j.seppur.2018.08.076.

Mika, T.S., Fuerstenau, D.W., 1969. A microscopic model of the flotation process, in: Proceedings of the VIII International Mineral Processing Congress, Leningrad. pp. 246–269.

Mohanty, S., 2009. Artificial neural network based system identification and model predictive control of a flotation column. Journal of Process Control 19, 991–999. URL: http://dx.doi.org/10.1016/j.jprocont.2009.01.001, doi:10.1016/j.jprocont.2009.01.001.

Moolman, D., Aldrich, C., Van Deventer, J., 1995a. The analysis of videographic data with neural nets. Chimica Acta Slovenica 42, 137–142.

Moolman, D., Aldrich, C., Van Deventer, J., Stange, W., 1994. Digital image processing as a tool for on-line monitoring of froth in flotation plants. Minerals Engineering1 7, 1149–1164. doi:10.1016/0892-6875(94)00058-1.

Moolman, D.W., Aldrich, C., van Deventer, J.S., Stange, W.W., 1995b. The classification of froth structures in a copper flotation plant by means of a neural net. International Journal of Mineral Processing 43, 193–208. doi:10.1016/0301-7516(95)00003-V.

Moolman, D.W., Aldrich, C., Schmitz, G.P., Van Deventer, J.S., 1996. The interrelationship between surface froth characteristics and industrial flotation performance. Minerals Engineering 9, 837–854. doi:10.1016/0892-6875(96)00076-3.

Moolman, D.W., Aldrich, C., Van Deventer, J.S., 1995c. The monitoring of froth surfaces on industrial flotation plants using connectionist image processing techniques. Minerals Engineering 8, 23–30. doi:10.1016/0892-6875(94)00099-X.

Moolman, D.W., Aldrich, C., Van Deventer, J.S., Bradshaw, D.J., 1995d. The interpretation of flotation froth surfaces by using digital image analysis and neural networks. Chemical Engineering Science 50, 3501–3513. doi:10.1016/0009-2509(95)00190-G.

Mular, A.L., 1972. Empirical modelling and optimization of mineral processes. Mineral Science and Engineering .

Neethling, S., Brito-Parada, P., Hadler, K., Cilliers, J., 2019. The transition from first to zero order flotation kinetics and its implications for the efficiency of large flotation cells. Minerals Engineering 132, 149–161. doi:10.1016/J.MINENG.2018.11.039.

Neethling, S., Cilliers, J., 2009. The entrainment factor in froth flotation: Model for particle size and other operating parameter effects. International Journal of Mineral Processing 93, 141–148. doi:10.1016/J.MINPRO.2009.07.004.

Neethling, S., Lee, H., Cilliers, J., 2002. A foam drainage equation generalised for all liquid contents. J. Phys. Condens. Matter 14, 331–342.

Neethling, S.J., Brito-Parada, P.R., 2018. Predicting flotation behaviour âĂŞ The interaction between froth stability and performance. Minerals Engineering 120, 60–65. doi:10.1016/j.mineng.2018.02.002.

Neethling, S.J., Cilliers, J.J., 2002. Solids motion in flowing froths. Chemical Engineering Science 57, 607–615.

Neethling, S.J., Cilliers, J.J., 2008. Predicting air recovery in flotation cells. Minerals Engineering 21, 937–943. doi:10.1016/j.mineng.2008.03.011.

Neethling, S.J., Cilliers, J.J., Woodburn, E.T., 2000. Prediction of the water distribution in a flowing foam. Chemical Engineering Science 55, 4021–4028.

Neethling, S.J., Lee, H.T., Cilliers, J.J., 2003. Simple relationships for predicting the recovery of liquid from flowing foams and froths. Minerals Engineering 16, 1123–1130. doi:10.1016/j.mineng.2003.06.014.

Nesset, J.E., Hernandez-Aguilar, J.R., Acuna, C., Gomez, C.O., Finch, J.A., 2006. Some gas dispersion characteristics of mechanical flotation machines, in: Minerals Engineering, pp. 807–815. doi:10.1016/j.mineng.2005.09.045.

Nguyen, A.V., Ralston, J., Schulze, H.J., 1998. On modelling of bubble-particle attachment probability in flotation. International Journal of Mineral Processing 53, 225–249. doi:10.1016/S0301-7516(97)00073-2.

Niemi, A.J., Ylinen, R., Hyötyniemi, H., 1997. On characterization of pulp and froth in cells of flotation plant. International Journal of Mineral Processing 51, 51–65. doi:10.1016/s0301-7516(97)00042-2.

Oosthuizen, D.J., Craig, I.K., 2019. Predicting optimal operating points by modelling different flotation mechanisms. IFAC-PapersOnLine 52, 60–65. doi:10.1016/j.ifacol.2019.09.164.

Oosthuizen, D.J., Craig, I.K., Jämsä-Jounela, S.L., Sun, B., 2017. On the current state of flotation modelling for process control. IFAC-PapersOnLine 50, 19–24. doi:10.1016/j.ifacol.2017.12.004.

Osorio, D., Pérez-Correa, J.R., Cipriano, A., 1999. Assessment of expert fuzzy controllers for conventional flotation plants. Minerals Engineering doi:10.1016/S0892-6875(99)00120-X.

Perez-Correa, R., Gonzalez, G., Casali, A., Cipriano, A., Barrera, R., Zavala, E., 1998. Dynamic modelling and advanced multivariable control of conventional flotation circuits. Minerals Engineering 11, 333–346. doi:10.1016/s0892-6875(98)00012-0.

Pitt, J., 1968. The development of systems for continuous optimal control of flotation plants by computer, in: System Dynamics and Automatic Control in Basic Industries (IFAC Symposium), Sydney. pp. 165–171.

Polat, M., Chander, S., 2000. First-order flotation kinetics models and methods for estimation of the true distribution of flotation rate constants. International Journal of Mineral Processing 58, 145–166. doi:10.1016/S0301-7516(99)00069-1.

Prakash, R., Majumder, S.K., Singh, A., 2018. Flotation technique: Its mechanisms and design parameters. Chemical Engineering and Processing - Process Intensification 127, 249–270. doi:10.1016/j.cep.2018.

03.029.

Putz, E., Cipriano, A., 2015. Hybrid model predictive control for flotation plants. Minerals Engineering 70, 26–35. doi:10.1016/j.mineng.2014.08.013.

Qin, S., Badgwell, T.A., 1997. An overview of industrial model predictive control technology. Control Engineering Practice doi:10.1.1.52.8909.

Riquelme, A., Desbiens, A., Del Villar, R., Maldonado, M., 2016. Predictive control of the bubble size distribution in a two-phase pilot flotation column. Minerals Engineering 89, 71–76. doi:10.1016/j.mineng.2016.01.014.

Rojas, D., Cipriano, A., 2011. Model Based Predictive Control of a Rougher Flotation Circuit Considering Grade Estimation in Intermediate Cells. Technical Report. Universidad Nacional de Colombia. Medellin. URL: http://www.redalyc.org/articulo.oa?id=49622365004{%}0AHow.

Rossiter, J., 2003. Model Based Predictive Control: A Practical Approach. Control Series.

Sbarbaro, D., del Villar, R., 2010. Advanced control and supervision for mineral processing. Advances in Industrial Control. doi:10.1007/978-1-84996-106-6.

Schubert, H., 2008. On the optimization of hydrodynamics in fine particle flotation. Minerals Engineering 21, 930–936. doi:10.1016/j.mineng.2008.02.012.

Shean, B., Hadler, K., Cilliers, J.J., 2017. A flotation control system to optimise performance using peak air recovery. Chemical Engineering Research and Design 117, 57–65. doi:10.1016/j.cherd.2016.10.021.

Shean, B., Hadler, K., Neethling, S., Cilliers, J.J., 2018. A dynamic model for level prediction in aerated tanks. Minerals Engineering 125, 140–149. doi:10.1016/j.mineng.2018.05.030.

Shean, B.J., Cilliers, J.J., 2011. A review of froth flotation control. International Journal of Mineral Processing 100, 57–71. doi:10.1016/j.minpro.2011.05.002.

Smith, H., Lewis, C., 1969. Computer control experiments at Lake Dufault. Can. I.M.M. Bulletin 62, 109–115.

Sontag, E., 1981. Nonlinear regulations: the piecewise linear approach. IEEE Transitions on Automatic Control 26, 346–358. doi:10.1109/TAC.1981.1102596.

Tian, Y., Luan, X., Liu, F., Dubljevic, S., 2018. Model Predictive Control of Mineral Column Flotation Process. Mathematics 6, 100. doi:10.3390/math6060100.

Varbanov, R., Forssberg, E., Hallin, M., 1993. On the modelling of the flotation process. International Journal of Mineral Processing 37, 27–43. doi:10.1016/0301-7516(93)90003-S.

Ventura-Medina, E., Cilliers, J.J., 2000. Calculation of the specific surface area in flotation. Minerals Engineering 13, 265–275. doi:10.1016/S0892-6875(00)00006-6.

Verbist, G., Weaire, D., Kraynik, A.M., 1996. The foam drainage equation. Journal of Physics Condensed Matter 8, 3715–3731. doi:10.1088/0953-8984/8/21/002.

Veselý, V., Rosinová, D., 2010. Robust Model Predictive Control Design, in: Zheng, T. (Ed.), Model Predictive Control, pp. 217–248. doi:10.5772/256.

Vinnett, L., Yianatos, J., Alvarez, M., 2014. Gas dispersion measurements in mechanical flotation cells: Industrial experience in Chilean concentrators. Minerals Engineering doi:10.1016/j.mineng.2013.12.006.

Wang, G., Ge, L., Mitra, S., Evans, G.M., Joshi, J.B., Chen, S., 2018. A review of CFD modelling studies on the flotation process. doi:10.1016/j.mineng.2018.08.019.

Wang, L., Peng, Y., Runge, K., Bradshaw, D., 2015. A review of entrainment: Mechanisms, contributing factors and modelling in flotation. doi:10.1016/j.mineng.2014.09.003.

Wang, W., Bergholm, F., Yang, B., 2003. Froth delineation based on image classification. Minerals Engineering 16, 1183–1192. doi:10.1016/j.mineng.2003.07.014.

Whiten, W., 1972. Simulation and model building for mineral processing. Ph.D. thesis. University of Queensland.

Yianatos, J.B., Bergh, L.G., 1995. Troubleshooting industrial flotation columns. Minerals Engineering doi:10.1016/0892-6875(95)00121-2.

Yoon, R.H., Mao, L.Q., 1996. Application of extended DLVO theory .4. Derivation of flotation rate equation from first principles. Journal of colloid and interface science 181, 613–626. doi:10.1006/jcis.1996.0419.

Zaragoza, R., Herbst, J.A., 1989. Model-based feedforward control scheme for flotation plants. Minerals and metallurgical processing , 177–185.

Table A1: Control variables most commonly used in MPC for flotation.

Study	**Input variables**		**Output variables**	
	Manipulated	**Disturbances**	**Controlled**	**Internal states**
Zaragoza and Herbst (1989)	Set points of the regulatory control loops	Flotation feed disturbances in the first cells of the circuit (using Kalman filter)	Pulp level	Mass of chalcopyrite in the pulp and froth phases Mass of locked particles in the pulp and froth phases Mass of gangue in the pulp and froth phases Mass of free pyrite in the pulp and froth phases Volume of liquid in pulp and froth phases (in cell 1 and 2)
Perez-Correa et al. (1998)	Collector doses Frother addition rate Pulp level set point	Copper head grade Feed flowrate Average feed particle size Iron feed content Feed pH	Concentrate grade Tailings grade Metallurgical recovery	Not reported explicitly
Maldonado et al. (2007a)	Output control valve of tailings flowrate Wash-water flowrate set point Air flowrate set point	Not reported explicitly	Froth depth Bias rate Gas hold-up	Not reported explicitly
Maldonado et al. (2007b)	Output control valve of tailings flowrate from each bank	Not reported explicitly	Pulp level at the bank j	Tailings grade Cumulative concentrate solid mass flowrate Grade in the concentrate
Maldonado et al. (2009)	Output control valve of tailings flowrate Wash water flowrate set point Air flowrate set point	Not reported explicitly	Froth depth Bias rate Collection zone gas hold-up	Not reported explicitly
Maldonado et al. (2010)	Superficial water velocity set point	Changes on superficial gas velocity Frother concentration	Sauter mean diameter	Not reported explicitly
Putz and Cipriano (2015)	Output control valve of tailings flowrate from each bank	Feed flowrate Copper head grade	Pulp level Final tailings grade	Not reported explicitly
Tian et al. (2018)	Feed velocity set point	Not reported explicitly	Mass concentration of solid particles in the air phase of froth overflow	Not reported explicitly